

**Th-AM-Sym1 MECHANICAL AND BIOCHEMICAL EVIDENCE FOR BINDING OF  $P_i$  TO A FORCE-GENERATING  $AM \cdot ADP$  STATE OF THE CROSS-BRIDGE CYCLE** J.A.Dantzig<sup>+</sup>, Y.E.Goldman<sup>+</sup>, D.R.Trentham<sup>+</sup>, M.R.Webb<sup>+</sup> & M.Yamakawa<sup>+</sup> Dept. of Physiol<sup>+</sup>, School of Med., Univ. of Penna., Phila., PA 19104 and Nat. Inst. Med. Res., Mill Hill, London NW7 1AA, U.K.

Mechanical and biochemical experiments on rabbit psoas muscle fibers suggest that during contractions, binding of inorganic phosphate ( $P_i$ ) to a force-generating acto-myosin-ADP cross-bridge state ( $AM \cdot ADP$ ) to form  $AM \cdot ADP \cdot P_i$  reduces force and facilitates cross-bridge detachment (Hibberd et al. *Science* 228:1317, 1985; Webb et al. *JBC* 261:15557, 1986). This links  $P_i$  release with force development. 10 mM  $P_i$  reduces active tension by ~25% but only reduces the ATPase rate by ~10% (Webb, et al., *ibid.*; Kawai et al. *Pflügers Archiv* In Press, 1986). Oxygen exchange experiments on contracting rabbit fibers indicate that  $P_i$  binds to  $AM \cdot ADP$  at the catalytic site with apparent second order rate constant  $\sim 500 M^{-1} s^{-1}$ , but mechanical experiments using photolysis of caged ATP suggest a 3 - 10 fold higher rate constant. In insect flight muscle fibers, oxygen exchange experiments suggest that the predominant steady-state intermediate is  $AM \cdot ADP \cdot P_i$  (Lund et al. *J. Musc. Res. & Cell Mot.* 6:665, 1985). However,  $P_i$  suppresses stretch activation and markedly accelerates relaxation from rigor by photolysis of caged ATP. Tension traces starting from different rigor force levels do not converge with a common final time course following caged ATP photolysis in insect fibers at 0  $P_i$  (Yamakawa et al. *Biophys. J.* 47:288a, 1985) but do converge at 10 mM  $P_i$ . Thus in vertebrate and insect fibers, mechanical measurements suggest a higher rate of  $P_i$  binding than fiber biochemical studies. These differences may be explained if  $P_i$  binds preferentially to cross-bridges in the  $AM \cdot ADP$  state when they bear a high force. Supported by MDA, MRC U.K., and NIH grants HL15835 to PMI and AM26846.

**Th-AM-Sym2 STUDIES ON WEAKLY- AND STRONGLY-BINDING CROSSBRIDGES: RELATING MUSCLE BIOCHEMISTRY TO FIBER PHYSIOLOGY.** M. Schoenberg, LPB, NIAMS, NIH, Bethesda, MD 20892

When strongly-binding crossbridges such as those in rigor or with MgADP at the active site are attached to actin, they detach with rate-constants slower than  $0.01 s^{-1}$ . In contrast, we have demonstrated in relaxed fibers a second type of attached crossbridge, the so-called "weakly-binding rapid-equilibrium" crossbridge. These crossbridges, which have many properties in common with the  $SIATP$  and  $SIADP \cdot P_i$  states seen in solution, exhibit a rapid equilibrium between attached and detached moieties, with detachment rate-constants greater than  $10^4 s^{-1}$ . Recently, we have been able to measure the ionic strength dependence of the attachment and detachment rate-constants of the weakly-binding MATP crossbridges in both skinned rabbit and frog fibers. The results suggest a number of correlations between the behavior of the crossbridge in fibers and that of acto-SI in solution. The significance of this with regard to the regulation of contraction in vertebrate skeletal muscle will be discussed.

We have also determined the attachment and detachment rate-constants for the crossbridge having non-hydrolyzable ATP analogues such as MgAMP-PNP and MgPP<sub>i</sub> bound at the active site. Since these rate-constants are slower than those with ATP, a very detailed comparison between solution and fiber is possible. In the fiber, the detachment of crossbridges with analogue bound is a multiexponential process. The fastest detachment rate-constants are comparable to the rate-constant for detachment of SI from actin in solution, but the majority are considerably slower. In addition, the analogue concentration dependence of the detachment rate-constants in the fiber is not described by the simple Michaelis-Menton expression. Mechanisms that might possibly account for this interesting divergence between solution and fiber will be explored and discussed.

**Th-AM-Sym3 MOLECULAR APPROACHES & MYOSIN STRUCTURE & FUNCTION.** James Spudich, Stanford University Medical Center, Stanford, CA.

**Th-AM-Sym4** SPECTROSCOPIC PROBES OF MUSCLE CROSS-BRIDGE ORIENTATION AND DYNAMICS. David D. Thomas, Department of Biochemistry, University of Minnesota, Minneapolis, MN 55455.

My coworkers and I have used both magnetic resonance and optical spectroscopy to study the orientations and rotational motions of probes attached to myosin heads, the globular ATP-splitting and actin-binding components of muscle cross-bridges. Our goal is to test and refine models for the role of myosin head rotation in force generation in vertebrate skeletal muscle. Experiments performed on purified myosin help define the degrees of rotational freedom (segmental flexibility) that are available to myosin. The selective labeling of myosin heads in intact muscle fibers extends these measurements to the active muscle fiber, permitting us to ask what motions may be coupled to force generation, and producing sensitivity to orientation as well as to rotational motion. Our results show that myosin heads rotate flexibly relative to the rest of myosin in the microsecond time range, with two degrees of rotational freedom that we assign to two proposed "hinges" within the cross-bridge. This rotational freedom is present in purified myosin and in relaxed muscle, but is rigidly restricted when myosin heads interact with actin in the absence of ATP, giving rise to a population of nearly uniformly oriented probes in rigor. During contraction, most of the probes are nearly as mobile as in relaxation. Transient experiments using caged ATP and isolated heads attached to actin suggest that some of the observed mobility may arise from cross-bridges attached to actin during the process leading to force generation. The correlation of spectroscopic signals with stiffness measurements in the presence of ATP analogs indicates that crossbridges can be attached stiffly by one head, with considerable heterogeneity in the stiffness and affinity of attachment.

**Th-AM-A1 THE CAUSE OF THE FAILURE OF THE "INDEPENDENCE PRINCIPLE."** Tobias L. Schwartz, Molecular and Cell Biology, University of Connecticut, Storrs, CT 06268.

It is demonstrated that the frequent collapse of equations based on the independence principle is linked to the failure of conditions of which we were warned by the original authors of the principle: "if, for instance, a change in  $c_1$  alters the form of the electric field in the membrane and therefore alters  $M_2$ ; in this case Equations (8) and therefore (12) are not obeyed." (pg. 468, Hodgkin, A.L. and A.F. Huxley, 1952. Measurement of current-voltage relations in the membrane of the giant axon of *Loligo*. J. Physiol. (London), 116:424-448.) This cautionary note seems to have been disregarded in later work. Indeed, the failure of this principle has nothing at all to do with, as has often been suggested, problems regarding the appearance of discrete intramembrane events and the use of a continuum diffusion theory. Thus: for example, a bilayer of 60 Å width is only an order of magnitude larger than the ionic diameters, and its molecular constituents will not be "blurred" into a continuum." (pg. 230, Starzak, M.E., 1984. The Physical Chemistry of Membranes. Academic Press. 334 pp..) Data will be presented that demonstrate the source of the failure to lie in the assumption that permeability is independent of the external concentration of the permeant species, and of the details of the intramembrane electrical potential.

**Th-AM-A2 EVIDENCE FOR A RESTING K CHANNEL IN THE SQUID AXON.** D.C. Chang, Department of Physiology and Molecular Biophysics, Baylor College of Medicine, Houston, TX 77030

The resting membrane of the nerve cell has a higher permeability to  $K^+$  ions than to  $Na^+$  ions. However, it is not clear whether such selectivity is determined by the number of excitable K and Na channels that remain open at the resting state, or whether there exists a different type of "resting channel" which is selectively permeable to  $K^+$  ions. Using a combination of voltage-clamp and internal perfusion techniques, we have conducted a series of experiments on the squid axon to examine this question. Our study indicated that the properties of the resting channel differ significantly from those of the delayed rectifier or the excitable Na channel. First, the resting channel has different pharmacological properties. When the Na channel and delayed rectifier K channel were blocked by TTX (tetrodotoxin) and TEA (tetraethylammonium) respectively, the axon still gave normal resting potential which varied with the external K concentration in a manner similar to that of an untreated axon. Second, our voltage-clamp measurements showed that the resting current remained unchanged when either the excitable Na channel or the delayed rectifier were blocked. Third, although the resting channel is most permeable to  $K^+$ , the ion-selectivity sequence for the resting channel differed quantitatively from that of the delayed rectifier. Fourth, the resting channel was found to be activated at a much lower membrane potential than that of the delayed rectifier. Fifth, varying the ionic environment has different effects on the resting channel and the delayed rectifier. For example, substitution of external  $Na^+$  by  $Rb^+$  increased the resting channel conductance but decreased that of the delayed rectifier. (Work supported in part by ONR contract N00014-85-K-0424 and NSF grant BNS-84-06932.)

**Th-AM-A3 POTASSIUM CHANNELS FROM SQUID RETINAL NERVE.** R. M. Torres and M. Condrescu. (Intr. by M. Barish). Department of Physiology, UCLA, Los Angeles, Ca 90024 and Instituto Venezolano de Investigaciones Cientificas, Apartado 21827, Caracas 1020 A Venezuela.

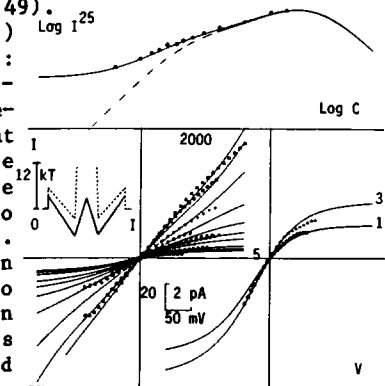
The retinal nerves of the squid have been demonstrated to be a high yielding source of axonal membrane (Condrescu et al. B.B.A. 769, 1984, 261-269) Its low traces of subcellular organelles, no myelin contamination and a favorable ratio of axonal over glial membranes make them well suited for channel extraction. Retinal nerves of several squids were dissected and homogenized, centrifugated and finally spinned down a discrete sucrose gradient. The interphase was collected and resuspended in  $K^+$  buffer. Care was taken to always keep the preparation in the presence of Potassium and to minimize Calcium concentration. A homogeneous population of unilamellar synthetic lipids vesicles were prepared using POPE and POPS (4:1 ratio) and Octyl Glucoside followed by dialysis (Mimms et al. Biochemistry 1981, 20, 833-840). Finally the natural membrane vesicles and the synthetic lipids vesicles were fused together by the freeze-thaw method followed by a mild sonication in order to decrease the number of channels per vesicle. The vesicles were fused to a planar bilayer of POPE painted in a teflon partition. Several types of unitary events were observed, the most conspicuous among them being a voltage-dependent 30 pS Potassium selective channel ( $P_K > P_{Na} > P_{Cl}$ ), a voltage-dependent 60 pS Ba-blockable non selective cationic channel, and a voltage-dependent 100 pS channel blocked by 5 mM TEA in a voltage-dependent fashion and only from one side. It is not yet known whether these channels are a representative profile of the population of channels in the retinal nerve axons or whether they have somehow been transformed during the extraction process. Anionic V-dependent and non V-dependent Cl-selective channels were also observed during some experiments. Supported by UPHS grant GM 30376.

**Th-AM-A4** A NEW INTERPRETATION OF THE EFFECTS OF QUATERNARY AMMONIUM ION DERIVATIVES ON POTASSIUM CHANNELS IN SQUID AXONS. John R. Clay, Lab. of Biophysics, NIH, Woods Hole, MA 02543.

I have recently demonstrated that blockade of potassium channels in squid axons by tetraethylammonium ions ( $\text{TEA}^+$ ) is independent of channel gating, in contrast to the original model of Clay Armstrong (J. Gen. Physiol. 50:491, 1966), which requires channel gates to open before blockade can occur (J.R. Clay, Biophys. J. 48:885, 1985; 49:216a, 1986). This new interpretation is based primarily on tail current kinetics. In the Armstrong model  $\text{TEA}^+$  must leave the channel before the channel gates can close. Consequently, blockade of inward (tail) current should be accompanied by a significant slowing of the tail current time course. Tail current kinetics are not modified if blockade is independent of gating, which is consistent with my experimental results. An additional test of these models is provided by a double pulse experiment in which the membrane potential is stepped to a depolarized level for a fixed period of time followed by a return to holding level for a variable period of time, and then stepped back to the depolarized level. If  $\text{TEA}^+$  has to leave the channel before the gates can close, then it might sometimes be trapped in the channel by the gates at the holding level, which would be manifested by a reduction in outward current with the second depolarizing step. This effect was not observed, which is consistent with my interpretation of  $\text{TEA}^+$  blockade. I have obtained qualitatively similar results with  $\text{C}_1$  and  $\text{C}_3$  ( $\text{TEA}^+$  is  $\text{C}_2$  in this terminology). However,  $\text{C}_4$  and  $\text{C}_5$  significantly slow tail currents, as predicted by the Armstrong model, and they each have a relatively long time constant for removal of blockade, as revealed by the double pulse protocol. Consequently, a seemingly minor change in the structure of an ionic blocker can produce a marked, qualitatively different mechanism of channel blockade.

**Th-AM-A5** SURFACE CHARGE IN A BARRIER MODEL CAN EXPLAIN THE LOW CONCENTRATION I-V BEHAVIOR OF THE  $\text{Ca}^{++}$ -ACTIVATED  $\text{K}^+$  CHANNEL. A. Villarroel and G. Eisenman. Physiol. Dept. UCLA Medical School, L.A., CA 90024. (Supp. by NSF (BNS 8411033) and USPHS (GM 24749)).

We measured I-V's of single Ca-activated K channels (rat t-tubule) in POPC/POPE bilayers in symmetrical 1-2000 mM K solutions and find: 1. The shape for outward I below 3 mM is extremely sublinear, indicating a zero voltage dependence of the entry step. 2. Despite the symmetry of I-V shape at high conc., an asymmetry (rectification) is seen at low conc. (cf. I-V's at 5-2000 mM with those at 1 and 3 mM). 3. The current at 25 mV ( $I^{25}$ ) becomes conc.-independent at low conc. (see log-log plot of data points from 1-2000 mM) instead of proportional to conc. (dashed line), confirming Vergara et al (Biophys. J. 45:73). Such behavior is expected if a negative surface charge were present in the vestibules; and we therefore extended the 3B2S barrier model to include the effects of surface charge in the vestibules (Gouy-Chapman approx.). Solid curves are expectations for outer and inner vestibules having 1 negative charge per 2360 and 5480  $\text{Å}^2$ , respectively (dashed curve is for zero charge). The rectification at low conc. results from surface charge asymmetry. Varying the barrier locations, the best fit occurs for zero V-dependence of entry. An asymmetrical surface charge always improves the fit. The fit shown is the best we obtain assuming interactions inversely proportional to distance, locations of the barriers and sites fixed, and allowing 5 energies, 2 surface charges, and 1 interaction parameter to vary.



**Th-AM-A6** IMPORTANT AMINO ACIDS ON THE EXTERNAL SURFACE OF POTASSIUM CHANNELS. Sherrill Spires and Ted Begenisich, Dept. of Physiology, Univ. of Rochester, Rochester, NY 14642.

We have continued our identification of chemical groups important for the proper function of potassium channels in squid giant axons. K channel ionic currents with elevated external K concentration were measured using the axial wire voltage clamp technique. We have previously reported that the histidine modifying reagent diethyl pyrocarbonate (DEP) slowed the activation kinetics of K channel ionic currents with little or no effect on the kinetics of the "tail" currents. While DEP reacts preferentially with histidyl residues on most model peptide systems reactions with amino groups have also been described. Histidine but not amino groups can be modified by photooxidation. Treatment of axons with the photosensitizing dye rose bengal (10 to 25  $\mu\text{M}$ ) also slows activation but not deactivation of K channels as reported by Bookman (Biophys. J. 45:144a, 1984). These results support the involvement of a histidine group(s) in the opening but not the closing of K channels. As another control for identification of the effects produced by DEP as arising from the reaction of this compound with histidyl residues, we also treated axons with the amino group-specific reagents SITS (1 mM) and TNBS (2.5 mM). Both compounds increased K channel currents. In addition TNBS slowed the activation kinetics; SITS had little or no effect on K channel kinetics. These results suggest modification of amino groups increases K channel currents. The kinetic effect produced by TNBS may be due to the alteration of another chemical group (e.g. sulfhydryl) or, more interestingly, to the different charge of the modified amino groups. The histidyl and amino groups identified in these experiments are probably on different regions of the K channel protein since DEP modification persists even after TNBS treatment. Support by USPHS grant NS-14138.

**Th-AM-A7 INTRACELLULAR CALCIUM MODULATES THE POTASSIUM CONDUCTANCE IN DIALYZED SQUID AXONS.** E. Perozo and F. Bezanilla. *Instituto Venezolano de Investigaciones Cientificas, Apartado 21827 Caracas 1020A, Venezuela and Department of Physiology, UCLA, Los Angeles, CA 90024.*

In voltage clamped squid axons dialyzed with 0  $Ca_i$ , addition of micromolar amounts of ionized calcium leads to an increase in the amplitude and a slowing down of the kinetics of the total outward current, closely resembling the modulation of K currents by ATP. (Biophys. J. 47:222a, 1985 and 49:215a, 1986). The internal dialysis solution contains in mM: 310 K, 30 phosphate, 4 Mg, 110 glycine, 1 EGTA and/or 10 BAPTA, pH=7.3; the external solution was artificial sea water containing 300 nM TTX and 1 mM cyanide. At the holding potential (HP) of -55 mV calcium alone produces an increase of up to three times in  $g_K$  with a  $K_{1/2}$  close to 1  $\mu$ M. The currents also turn on more slowly than the control. The Ca effect is voltage dependent since the magnitude of the total stimulation is diminished at more negative HP. However, we found an increase in maximum  $g_K$  even when slow inactivation was removed with a negative holding potential, implying that part of the increase in  $g_K$  corresponds to the activation of an additional ionic conductance. The stimulation of  $g_K$  is partially blocked by external application of charybdotoxin (CTX) or TEA, suggesting the presence of a Ca-activated K channel. Apamin has no effect. Strontium can elicit a Ca-like response but with less affinity. These effects cannot be explained assuming a modification of a negative surface charge in the axoplasmic side since it is not possible to superimpose current records with and without calcium at two different voltages. The similarities of the Ca effects with ATP potentiation of  $g_K$  are striking since the ATP effect is also blocked in the same manner by external CTX and TEA. We propose that the squid axon has a Ca-activated K channel in addition to the classical delayed rectifier and that both are modulated by ATP phosphorylation. Supported by MDA and USPHS grant GM30376. E.P. was a Grass fellow.

**Th-AM-A8 CALCIUM- AND VOLTAGE-DEPENDENT  $K^+$  CHANNELS IN A MOLLUSCAN PHOTORECEPTOR.** J. Farley, Prog. in Neurosci., Princeton Univ., Princeton, NJ 08544.

A voltage- and calcium-dependent  $K^+$  current ( $I_{K-Ca}$ ) plays a crucial role in determining the magnitude of the steady-state depolarizing generator potential of *Hermisenda* Type B photoreceptors' response to light. Although well described at the macroscopic current level, little information is available concerning the single-channel properties of  $I_{K-Ca}$  channels.

Single-channel potassium currents were recorded from *Hermisenda* Type B photoreceptor soma membranes in cell-free and cell-attached recording configurations. Similar, if not identical, channels were incorporated into artificial bilayer membranes formed on the tips of patch clamp electrodes, from crude homogenates of entire *Hermisenda* nervous systems as well as from homogenates of just eyes. The channels detected were voltage-dependent: in excised patch and in bilayer recordings, at a free calcium concentration of  $10^{-6}$  M, the probability of the channel remaining in the open state increased as the membrane potential was made more positive. These channels were also calcium-dependent: at membrane potentials more positive than -20 mV, decreases in free calcium concentrations to less than  $10^{-7}$  M resulted in closure of the channels. Channels of the same unitary conductance and general pattern of activity were also routinely seen when pharmacological blockers of other voltage-dependent  $K^+$  channels, 4-AP and TEA, were present in the patch pipette. It is likely that these channels underly the TEA- and 4-AP resistant macroscopic calcium-activated potassium current of Type B photoreceptors which is selectively reduced by associative learning, serotonin and protein kinase C activation.

**Th-AM-A9 POTASSIUM GATING CURRENTS IN THE PERFUSED AXON ARE MODIFIED BY ATP.** C. Webb and F. Bezanilla. *Department of Physiology, UCLA, Los Angeles, Ca. 90024.*

We previously reported that ATP modulates K currents in the perfused and voltage-clamped squid giant axon (Biophys. J. 49:215a, 1986). Modulation of K gating currents is presented here. The standard internal perfusion medium (200KFG) contained (in mM): 160 K-glutamate, 40 KF, 10 Tris, and 2 Mg, pH 7.4 (19 to 20°C). For gating current recording, the internal medium (350Cs) contained 300 mM Cs-Glutamate and 50 mM CsF in place of the 160 mM K-Glutamate and 40 mM KF. Dibucaine (.25 mM) was added to the 350Cs and, on occasion, 30 mM TEA and/or 7  $\mu$ M 3,4-Diaminopyridine. ATP was added as ATP-Mg (2 mM) with 50 nM protein kinase (catalytic subunit of cAMP dependent from Sigma). The standard external medium (10KASW) contained (in mM): 10 KCl, 430 NaCl, 50 MgCl<sub>2</sub>, and 10 CaCl<sub>2</sub>, with 500 nM TTX, pH 7.6. The external medium for gating current recording (CsASW) contained 50 mM CsNO<sub>3</sub> and 440 mM TrisNO<sub>3</sub>, in place of the 10 mM KCl and 430 mM NaCl; in some cases 50 mM TEA was added. The experimental protocol was as follows: K currents were recorded (in 200KFG) first with 10KASW and then with CsASW; gating currents were recorded in 350Cs with CsASW; ATP and protein kinase were added to the 350Cs and gating currents were recorded; ATP and protein kinase were removed and the axon was washed in 350Cs for 15 min.; K currents were recorded in 200KFG first with CsASW and then with 10KASW. In most cases about 60 percent of the original ionic current was recovered upon returning to 200KFG. The ionic currents recorded before and after treatment with ATP were compared to determine the degree of phosphorylation. In the presence of ATP, the steady state charge-voltage curve (Qrel-V) was shifted by about 5 mV (in the depolarizing direction). The steady state activation curve, measured in CsASW, is about 35 mV depolarized to that of the Qrel-V curve in both the control situation and in the presence of ATP. The turn on time constant of the gating current was slower after phosphorylation, consistent with the increased lag in the turning on of the ionic currents in the presence of ATP. The time constant for turning off of the gating current was faster in the presence of ATP, also consistent with the ionic currents which turn off more quickly following phosphorylation. Supported by USPHS grant GM30376 and MDA.

**Th-AM-A10** GYCOLYTIC SUBSTRATES SUPPRESS THE ATP-SENSITIVE  $K^+$  CHANNEL IN HEART. James Weiss and Scott Lamp, UCLA School of Medicine, Los Angeles, CA 90024

During metabolic inhibition in heart, action potential shortening and  $K^+$  loss occur as a result of activation of the ATP-sensitive  $K^+$  channel ( $i_{K(ATP)}$ ) and are attenuated by enhanced glycolysis. To test whether glycolytic ATP production can suppress  $i_{K(ATP)}$ , we studied the effects of various substrates necessary for the ATP-producing steps of glycolysis on single channel recordings of  $i_{K(ATP)}$  in enzymatically isolated guinea pig ventricular myocytes using the patch clamp technique. In cell attached patches in freshly permeabilized (saponin-treated) cells, removal of ATP from the bath promptly activated  $i_{K(ATP)}$  (unitary conductance = 64 pS with symmetrical 150 mM KCl). The combination of phosphoenol pyruvate (PEP, 2 mM) and ADP (0.5 mM) were as effective as ATP in completely and reversibly suppressing  $i_{K(ATP)}$  within 60 s (10/11 patches), whereas PEP or ADP alone or pyruvate (2 mM) + ADP were ineffective ( $n = 4-6$ ). Fructose 1,6-diphosphate (2 mM), NAD (1 mM), ADP (0.5 mM), and  $P_i$  (1 mM) also completely suppressed  $i_{K(ATP)}$  ( $n = 3$ ). With the mitochondrial inhibitor FCCP (1  $\mu$ M) present, PEP + ADP still suppressed  $i_{K(ATP)}$ , indicating that glycolytic ATP production was sufficient to inhibit the channel. Inclusion of an ATP-consuming system (10 IU/cc hexokinase + 10 mM glucose) with PEP + ADP did not impair the ability of these substrates to completely suppress  $i_{K(ATP)}$  (3/3 patches), raising the possibility that glycolytically-derived ATP may not be freely diffusible in the cytosol. In excised inside-out patches, the above substrates were generally ineffective although in 1/9 patches PEP + ADP reversibly suppressed  $i_{K(ATP)}$ . These findings suggest that glycolytic enzymes are closely associated with  $i_{K(ATP)}$  in heart, and possibly provide a compartmentalized supply of ATP to this channel.

**Th-AM-A11**  $K^+$  CHANNELS IN MURINE B CELLS AND THEIR PRECURSORS ARE MODULATED BY cAMP. D. Choquet, P. Sarthou<sup>+</sup>, D. Primi<sup>+</sup>, P.A. Cazenave<sup>+</sup> & H. Korn<sup>+</sup>. INSERM U261<sup>+</sup> and Dpt of Immunology<sup>+</sup>, Institut Pasteur, 25 Rue du Dr. Roux, 75724 Paris Cédex 15.

We have used the whole-cell patch clamp technique to analyze ionic currents of LPS-stimulated spleen B cells and of pre-B cell lines, immortalized at representative stages of B cell development with Abelson Murine Leukemia virus. All these lymphocytes display a similar voltage-activated potassium current of the delayed rectifier type which is detectable above -40 mV, and exhibit voltage-dependent activation and inactivation kinetics (for instance, for a depolarizing pulse from -80 mV to 0 mV, the half-time to peak and half decay times were respectively:  $3.3 \pm 1.2$  ms,  $n = 14$  and  $317 \pm 93$  ms,  $n = 7$ ; 18-81 pre-B cell line). Although reduced by  $Co^{++}$  and  $Cd^{++}$  (1 mM), this current does not seem to be activated by  $Ca^{++}$  entry since it appears similar to the control when recorded in a medium containing no  $Ca^{++}$  and .5 mM EGTA. The maximum  $K^+$  conductance does not vary significantly among cell types ( $5.6 \pm 1.5$  nS, from a total of 115 cells belonging to 6 different lineages), thus suggesting a lack of obvious correlation between its presence and immunocompetency. Furthermore, its similarities with currents described by others in T-cells and their precursors seem to indicate that this  $K^+$  channel has developed before the divergence of discrete B and T cells lineages. In the light of understanding the physiological role of this channel, we have investigated whether it is modulated by second messengers. Increasing intracellular cAMP either by external addition of Forskolin or by direct inclusion of cAMP (1 mM) and theophylline (1 mM) in the recording pipette induces a marked decrease of the peak  $K^+$  current at all potentials, associated with increased rates of inactivation.

**Th-AM-A12** EFFECTS OF METABOLITES ON A  $K^+$  CHANNEL IN THE INSULIN-SECRETING B-CELL LINE, RIN m5F.

B. Ribalet, S. Ciani and G. Eddlestone. Dept. of Physiology, Ahmanson Laboratory of Neurobiology and JLNRC; UCLA, Los Angeles, CA 90024.

A  $K^+$  channel in membranes of the B-cell line, RIN m5F, was studied using the patch-clamp technique. In cell-attached patches, and for pipette solutions containing 140 mM KCl, the I-V curves exhibited inward rectification. The conductance (about 50 pS) was similar to that reported by Ashcroft et al. for B-cell of mature animals (1984, *Nature*, 312, 446). 5 mM glucose in the bath suppressed the channel activity, while .4 mM 2,4-DNP enhanced it, thus indicating a link between channel function and metabolism. Moreover, in excised inside-out patches, the fluctuations of a channel with similar conductive properties was inhibited by ATP in a dose-dependent mode, the half-maximal concentration being about 70  $\mu$ M; approximately five times the value found by Cook et al. for neonatal rat B-cells (1984, *Nature*, 311, 271). ADP also acted as a channel inhibitor, but with much lesser potency than ATP. However, with ADP present, the blocking efficacy of ATP was reduced, suggesting that the effects of the two nucleotides are not merely additive. In conclusion, it seems reasonable to argue that inhibition of the  $K^+$  channel activity by 5 mM glucose is indicative of a role for this channel in the early phase of the cell depolarization, but is inconsistent with its involvement in the regulation of the burst pattern, which occurs at higher glucose concentrations. In addition, since both ATP and ADP are present in these cells, the reduction by ADP of the effect of ATP in excised patches might help one to understand why, in intact cells, the channel is still active for intracellular ATP concentrations (3 to 5 mM) that, if present in a solution bathing the intracellular side of an excised patch, would completely inhibit it.

**Th-AM-B1 THREE CELLULAR MECHANISMS MAY CONTRIBUTE TO THE INOTROPIC EFFECT OF REDUCED TRANSMEMBRANE [Na] GRADIENT.** Donald M. Bers. Div. Biomed. Sci., Univ. of Calif., Riverside, CA 92521.

Reduction of the [Na] gradient in cardiac muscle increases the contractile force. This is often attributed in a general way to Na/Ca exchange. However, the direct mediator of the enhanced twitch may be increased: a) SR Ca release, b) Ca influx or c) resting free  $[Ca]_i$ . Increases of force in rabbit ventricular muscle were induced by [Na] gradient reduction (i.e. low  $[Na]_o$  or Na-pump inhibition by either acetylstrophanthidin (ACS) or low  $[K]_o$ ). Similar increases in contractile force (in response to [Na] gradient reduction) were also observed after pretreatment with 10 mM caffeine or 100-500 nM ryanodine. It is concluded that an intact functioning sarcoplasmic reticulum is not required for the inotropic effect of [Na] gradient reduction (although the SR may normally contribute to the inotropic response). Changes of interstitial [Ca] were measured using double-barreled extracellular Ca-selective microelectrodes. ACS (3-5  $\mu$ M) usually leads to an increase in the magnitude of  $Ca_o$  depletions associated with individual contractions. However, ACS can also lead to  $Ca_o$  accumulation during contractions and especially at potentiated contractions. This  $Ca_o$  accumulation can be suppressed by ryanodine and it is suggested that this apparent enhancement of Ca efflux is secondary to an enhanced release of Ca from the SR. Under conditions which minimize Ca efflux during contractions (i.e. with ryanodine and after a rest interval) ACS clearly increases the initial rate and extent of  $Ca_o$  depletions. Thus, ACS can increase both Ca influx and Ca efflux during the cardiac muscle contraction. A simple model describes the the direction of net Ca fluxes during the action potential based on changes of Na/Ca exchange reversal potential. Reduction of the [Na] gradient leads to net cellular Ca uptake (via Na/Ca exchange) and may elevate  $[Ca]_i$ . Thus while net Ca uptake may occur, three independent mechanisms may directly contribute to the increase in contractile force observed at individual contractions: 1) enhanced Ca influx 2) increased SR Ca release and 3) increased resting  $[Ca]_i$ .

**Th-AM-B2 MYOPLASMIC pH TRANSIENTS MONITORED WITH INDICATOR DYES IN FROG SKELETAL MUSCLE FIBERS.**

S. M. Baylor, S. Hollingworth and P. Pape (Intr. by B. G. Kennedy). Department of Physiology, University of Pennsylvania, Philadelphia, PA 19104.

Intact single fibers, mounted on an optical bench and stretched to long sarcomere spacing, were micro-injected with the pH indicator Phenol Red. Dye-related absorbance  $A(\lambda)$  ( $450 \text{ nm} < \lambda < 640 \text{ nm}$ ) had a spectral shape in myoplasm that was red-shifted by about 10 nm when compared with calibration curves measured in 140 mM KCl. Moreover, the average value of the apparent diffusion constant of the dye was  $0.38 \times 10^{-6} \text{ cm}^2/\text{s}$  ( $N=4, 16^\circ\text{C}$ ), a value about 4-5 times smaller than expected in myoplasm for a freely diffusible molecule the size of Phenol Red (MW 346). These findings are consistent with there being a major sub-population of dye molecules bound to myoplasmic constituents of larger molecular weight. In spite of the uncertainties raised by the presence of bound dye, the apparent pH of myoplasm,  $\text{pH}_{\text{app}}$ , as inferred from the shape of  $A(\lambda)$ , changed approximately in the manner expected when fibers were subjected to acid or alkaline loads by exposure to  $\text{CO}_2$  or  $\text{NH}_3$ , respectively.

In response to a single action potential, an absorbance change from Phenol Red,  $\Delta A(\lambda)$ , was detected, which had the spectral shape expected for a myoplasmic  $\Delta \text{pH}_{\text{app}}$ . The peak value of  $\Delta \text{pH}_{\text{app}}$  averaged +0.003 (pH units) and occurred about 10 ms after the peak of the myoplasmic  $\text{Ca}^{2+}$  transient, as estimated from fibers injected with Antipyrylazo III. The amplitude and time course of  $\Delta \text{pH}_{\text{app}}$ , through time to peak, can be accounted for if a proton flux from myoplasm to sarcoplasmic reticulum (SR) accounts for roughly 1/3 - 1/2 of the charge balance required to accompany SR  $\text{Ca}^{2+}$  release (cf. Somlyo et al., 1981; Baylor et al., 1982). Analogous experiments with the pH/Mg indicator Arsenazo I also revealed a  $\Delta A(\lambda)$  consistent with the  $\Delta \text{pH}_{\text{app}}$  inferred from Phenol Red. Supported by NS 17620.

**Th-AM-B3 FURA2 SIGNALS FROM INTACT FROG SKELETAL MUSCLE FIBERS.** S. Hollingworth and S. M. Baylor. Department of Physiology, University of Pennsylvania, Philadelphia, PA 19104.

Single fibers were mounted on an optical bench apparatus, stretched to long sarcomere spacing and micro-injected with membrane-impermeant Fura2 (Grynkiewicz, Poenie and Tsien, 1985). Absorbance and/or fluorescence signals were measured from the dye, both in resting and electrically stimulated fibers. The apparent diffusion constant of the dye,  $D_{\text{app}}$ , was  $0.36 \times 10^{-6} \text{ cm}^2/\text{s}$  ( $N=7, 16^\circ\text{C}$ ), a value about 3-fold smaller than expected in myoplasm, for a freely diffusible molecule the size of Fura2 (MW 636.5). The small value of  $D_{\text{app}}$  can be explained if approximately two-thirds of the dye is bound to muscle constituents of larger molecular weight. Measurements of fluorescence anisotropy confirmed that Fura2 in myoplasm is significantly less mobile than free dye in a salt solution.

In response to a single action potential, a transient increase in  $\text{Ca}^{2+}$ -Fura2 complex was detected, the time course of which was considerably slower than the myoplasmic  $\text{Ca}^{2+}$ -signal simultaneously measured from Antipyrylazo III. The slow response can be explained if the off-rate of the  $\text{Ca}^{2+}$ -Fura2 reaction in myoplasm is about  $25 \text{ s}^{-1}$ , a value 3-4 fold smaller than the off-rate reported in vitro. In fibers injected with large quantities of Fura2 (0.5-1.2 mM), the peak rate of  $\text{Ca}^{2+}$  release from the SR (sarcoplasmic reticulum) was estimated to be unchanged or increased, not decreased, in spite of the fact that changes in myoplasmic free  $[\text{Ca}^{2+}]$  were buffered significantly by Fura2. For example, the  $\text{Ca}^{2+}$ -signal simultaneously measured from Antipyrylazo III in these fibers was both reduced in amplitude and abbreviated in time course because of the large amount of  $\text{Ca}^{2+}$  (0.2-0.4 mM) transiently bound by Fura2. Assuming no pharmacological action of Fura2, these latter findings argue against a  $\text{Ca}^{2+}$ -induced release of  $\text{Ca}^{2+}$  as being the physiological trigger for SR  $\text{Ca}^{2+}$  release in skeletal muscle. Supported by NS 17620

**Th-AM-B4** THE CASE FOR CALCIUM STORE LEAK AS SPECIFIC RYANODINE (Ry) MECHANISM IN INTACT CARDIAC MUSCLE. Donald W. Hilgemann, Department of Physiology UCLA School of Medicine CHS A3-381, Los Angeles, CA 90024.

Extracellular calcium ( $[Ca]_o$ ) transient measurements have established 1) that Ca taken up by cardiac cells during excitation, returns only very slowly to the extracellular space during quiescence (time course on the order of minutes), 2) that progressive Ry pre-treatments ( $10^{-10}$  to  $10^{-6}$ M) progressively accelerate this time course (closely related to loss of contractility) down to seconds, and 3) that Ry strongly enhances cumulative  $[Ca]_o$  depletions at post-rest stimulation. Action 2) was exactly predicted by Ca store leak as Ry mechanism, but action 3) suggests "hyper-filling" of SR, consistent with inhibition of release. In order to produce rapid onset of Ry action, atria were stimulated by twin or triple pulses at 0.1 Hz basal rate (=large contractions, necessary for Ry action onset), and 0.2 mM Ry was added (~ 50000-fold effective concentration); during loss of contractility over 20 to 40 s,  $[Ca]_o$  increased from 200  $\mu$ M baseline to 230  $\mu$ M (tetramethylurexide measurements);  $[Ca]_o$  returned to baseline over 15 min (=time course of extracellular exchange). Caffeine application resulted in no further increment of  $[Ca]_o$ . During the reequilibration period, cumulative depletions could be evoked by stimulation bursts, but depletions were of smaller magnitude than Ry-induced Ca release. These results support the idea that the sarcoplasmic reticulum is unloaded by Ry in intact cardiac muscle. Old and new evidence for and against the suggestion of calcium leak as primary Ry action in intact muscle will be reviewed with the aid of computer simulations: 1) actions on interval-strength relationships; 2) actions in  $^{45}$ Ca-flux studies; 3) interactions with other interventions (e.g., caffeine).

**Th-AM-B5** HIGH AFFINITY EFFECT OF NIFEDIPINE ON K CONTRACTURE IN SKELETAL MUSCLE SUGGESTS A ROLE FOR CALCIUM CHANNELS IN EXCITATION-CONTRACTION COUPLING. R.F. Rakowski, E. Olszewska and C. Paxson. Dept. of Physiology and Biophysics, The Chicago Medical School, North Chicago, IL 60064.

Dihydropyridine binding sites from skeletal muscle t-tubules have been reconstituted and shown to form functional calcium channels (Flockerzi, et al., *Nature* 323:66 1986). However, the role of these calcium channels in excitation-contraction coupling is not known. We have studied the effect of nifedipine on K contractures in the cutaneous pectoris muscle of the frog. Experimental solutions of racemic nifedipine (Sigma) were prepared daily. Small bundles of 20-40 fibers were placed in normal frog Ringer's solution containing 2.5 mM K and 120 mM Cl. (Temp. 6-10°C). Muscles were pre-exposed to 10 mM K for 10 min prior to each contracture and then exposed to 100 mM K at constant KCl product. Exposure to 100 mM K was maintained until relaxation of the resulting K contracture was complete. 1  $\mu$ M nifedipine applied in the dark at the time of the pre-exposure to 10 mM K and maintained throughout the K contracture, had only a small effect on peak tension but blocked a second K contracture. Nifedipine block was reversible by warming the muscle to 20-22°C during a recovery period of 50 min in 2.5 mM K. Lower doses of nifedipine produce less complete block of the second K contracture. The data were fitted by 1:1 binding with an apparent  $K_D$  of 53 nM. Pre-exposure to 5K rather than 10K shifted the apparent  $K_D$  to the right and reduced the steepness of the dependence on nifedipine concentration. The ability of nifedipine to block K contractures is strongly temperature and voltage-dependent. The results suggest that nifedipine binds to inactivated t-tubular calcium channels and that reactivation of this protein is required for recovery from the mechanically refractory state.

**Th-AM-B6** A COMPARISON OF THE KINETICS OF CHARGE MOVEMENT AND ACTIVATION OF SR CALCIUM RELEASE DURING EXCITATION IN FROG SKELETAL MUSCLE. B. J. Simon and M. F. Schneider, Dept. of Biological Chemistry, University of Maryland School of Medicine, Baltimore, MD 21201 USA

We have monitored myoplasmic  $[Ca]$  transients using the calcium indicator Antipyrylazo III and intramembrane charge movement (Q) in cut segments of single frog twitch fibers voltage clamped in a double Vaseline gap chamber (8°C). The rate of SR calcium release (RREL) was calculated from the calcium transients (Melzer et al., *J. Physiol.* 373:481, 1986). During 200 ms depolarizing test pulses the rate of release rose to an early peak and then declined nearly exponentially to a final steady level of ~1/4 of the peak. If a large conditioning pulse preceded the test pulse the early peak of release could be completely suppressed, presumably due to the elevated  $[Ca]$  causing maximal Ca-induced inactivation (Simon et al, *J. Gen. Physiol.* 86:36a, 1985). The resulting test RREL rose monotonically to a final steady level essentially the same as the final level to which it decayed in the absence of the conditioning pulse. The time course of suprathreshold Q and "inactivated" RREL was compared using a pulse protocol in which test pulses to various potentials were immediately preceded by: (1) a 20 ms pulse to +50 mV to raise  $[Ca]$  and (2) a 50 ms pulse to a potential just subthreshold for calcium release. With this pulse protocol the time course of the test pulse Q and the "inactivated" RREL were found to be very similar, with release activation delayed by a few ms compared to Q. These results support the previous finding that suprathreshold Q and RREL corrected numerically for inactivation and depletion have a similar time course (Schneider and Simon, *Proc. Inter. Union Physiol. Sci.* XVI:265, 1986). Supported by NIH F32-AM07267 (BJS) and R01-NS23346.



**Th-AM-B7** SKELETAL MUSCLE EXCITATION-CONTRACTION COUPLING: TRANSVERSE TUBULE CONTROL OF SARCOPLASMIC RETICULUM  $Ca^{2+}$ -INDUCED  $Ca^{2+}$  RELEASE. Sue K. Donaldson, Esther M. Gallant, and Daniel A. Huetteman. Departments of Physiology and Veterinary Biology and School of Nursing, University of Minnesota, Minneapolis, MN 55455 USA.

The purpose of this study was to test whether changes in resting transverse tubule TT membrane potential alter the sensitivity or magnitude of sarcoplasmic reticulum (SR)  $Ca^{2+}$ -induced  $Ca^{2+}$  release (CaIR). Methods were as used previously (J.G.P. 86, 501) except that peeled skeletal muscle fibers from normal and malignant hyperthermic (MH) pigs were studied. CaIR is a secondary component of the  $Cl^{-}$ -induced  $Ca^{2+}$  release stimulated by ionic depolarization of sealed TTs in mammalian peeled fibers. The primary component of  $Cl^{-}$ -induced SR  $Ca^{2+}$  release is indistinguishable for MH and normal skeletal peeled fibers at all TT resting conditions and is graded by varying conditions of resting TT polarization and  $Cl^{-}$  stimulation consistent with intact fiber inactivation and activation curves. The  $[Ca^{2+}]$  threshold for secondary CaIR was lowered by resting TT depolarization in both normal and MH fibers. In addition, the magnitude of the secondary CaIR component was significantly larger in MH fibers at maximum  $Cl^{-}$  stimulation from normal resting TT conditions and it increased under resting TT depolarization conditions. Resting TT hyperpolarization conditions corrected the magnitude of the secondary CaIR component of MH fibers to normal. In summary, resting TT membrane potential appears to set the sensitivity of the SR CaIR in all skeletal muscle fibers. This TT-SR control mechanism may be defective in MH (see abstract, Gallant et al., 1987). [Supported by grants from MDA and NIH (AR 35132).]

**Th-AM-B8** SKELETAL MUSCLE EXCITATION-CONTRACTION COUPLING: PLASMALEMAL ALTERATION IN MALIGNANT HYPERTHERMIA. Esther M. Gallant and Sue K. Donaldson. Departments of Veterinary Biology and Physiology, and School of Nursing, University of Minnesota, St. Paul, MN 55108.

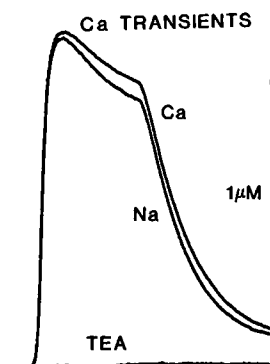
Muscles of malignant hyperthermia (MH) susceptible swine characteristically exhibit abnormal contractile responses in the absence of drugs, i.e., higher twitch-to-tetanus ratio (twitch ratio), and larger contractures in response to increased  $[K^{+}]$ . We hypothesized that these abnormal responses resulted from defective T-tubule (TT) control of sarcoplasmic reticulum (SR) calcium release at resting membrane potentials. Recently, (see abstract, Donaldson et al., 1987) hyperpolarization was shown to return abnormal ionic depolarization-induced responses of MH peeled fibers to normal levels. This led us to investigate whether hyperpolarization might also reverse abnormal contractile responses of intact MH muscle cells. Small bundles of cells intact from tendon to tendon were dissected from MH and normal porcine forelimb muscles. Exposure of muscle bundles to 2 mM  $K^{+}$  with constant  $[K^{+}][Cl^{-}]$  results in a 10 mV hyperpolarization and a significant ( $p < 0.01$ ) decrease in the twitch ratio of MH bundles ( $0.21 \pm 0.03$  to  $0.14 \pm 0.02$ ), but no change in the twitch ratio of normal bundles ( $0.13 \pm 0.01$  and  $0.12 \pm 0.01$ ). Hyperpolarization also reduced maximum  $K^{+}$ -contracture (150 mM  $K^{+}$ ) tension of MH bundles toward normal. There was no change in  $K^{+}$ -contractures of hyperpolarized normal bundles. Thus, two abnormal responses of intact MH muscle cells can be returned toward normal by surface membrane hyperpolarization. This supports our hypothesis that TT voltage control of SR calcium release may be defective in MH muscles. [Supported by the Muscular Dystrophy Association of America and NIH (AR 35132).]

**Th-AM-B9** MYOPLASMIC  $Ca^{2+}$  CONCENTRATION IN DYSTROPHIC HAMSTER. V. Sánchez<sup>1</sup>, S. Bhattacharya<sup>2</sup>, J.R. López<sup>1</sup>, F. Sreter<sup>3</sup>, J. Vergara<sup>4</sup>. <sup>1</sup>CBB, IVIC, Apartado 21827, Caracas, Venezuela, <sup>2</sup>Dept. Surgery, University of Tennessee, TN 33163. <sup>3</sup>Muscle Dept., BBRI, Boston, MA 02114 <sup>4</sup>Physiology Dept., UCLA, Los Angeles, CA 90024.

Duchenne muscular dystrophy has been associated to an elevated intracellular  $[Ca^{2+}]$  in skeletal muscle (Bertorini et al. Neurology (NY) 31:46, 1981). We have measured the free intracellular calcium concentration ( $[Ca^{2+}]_i$ ) in nondystrophic (BIO FIB strain) and dystrophic hamsters (BIO 14.6 strain) by means of  $Ca^{2+}$  selective microelectrodes (López et al. Biophys. J. 43:1, 1983). The animals were anesthetized with nembutal (0,02 grs intraperitoneally) and then the tibial anterior and the EDL were removed by careful dissection, and mounted on a temperature controlled bath (37°C) for the electrophysiological measurements. Individual muscle fibers were impaled first with the 3M KCl microelectrode to measure the resting membrane potential and then with the  $Ca^{2+}$  selective microelectrode to determine the  $[Ca^{2+}]_i$ . The resting intracellular  $Ca^{2+}$  concentration in non-dystrophic hamsters was  $0.11 \pm 0.01 \mu M$  (M + SEM) while it was  $0.43 \pm 0.02 \mu M$  in dystrophic hamsters. These results are the first direct demonstration that the resting myoplasmic  $[Ca^{2+}]_i$  is substantially higher in dystrophic hamsters than in control animals, and provides further support to the hypothesis about the role of  $Ca^{2+}$  in the pathophysiology of Duchenne muscular dystrophy. (Supported by CONICIT S1-1247, MDA).

**Th-AM-B10** A Ca-Mg-Na SITE MUST BE OCCUPIED FOR INTRAMEMBRANE CHARGE MOVEMENT AND CA RELEASE IN FROG SKELETAL MUSCLE. G. Brum, R. Fitts, G. Pizarro and E. Rios, (introduced by B. Eisenberg), Department of Physiology, Rush University, Chicago, IL 60612.

Ca release from the sarcoplasmic reticulum in muscle fibers under voltage clamp is smaller and more rapidly decaying in low extracellular Ca (Rios et al., *Biophys. J.* 47: 353a). Intramembrane charge movement at voltages positive to  $-70$  mV (charge 1) is also reduced in low Ca (Brum & Rios, *Biophys. J.* 49: 459a). We now report that Ca transients and charge 1 are essentially abolished in a medium containing TEA as the sole cation (record labeled TEA in the figure). Ca transients and charge movement are restored if any of the following ions is substituted isoosmotically for TEA: Ca (1.8 mM); Na (160 mM); Mg (16 mM) (not shown). In the absence of these ions the distribution of mobile charge with voltage is identical to that of a fiber inactivated by sustained depolarization (Brum & Rios, *Biophys. J.* 49: 12a) or nifedipine. In conclusion, a cation binding site, accessible from outside the cell, must be occupied for charge movement and Ca release. The site binds Ca, Mg and Na with approximate selectivity 100:10:1. Many observations on inactivation by depolarization or dihydropyridines can be explained if inactivation requires unbinding of the cation.



**Th-AM-B11** INOSITOL 1,4,5-TRISPHOSPHATE ( $\text{InsP}_3$ ) INDUCES CONTRACTIONS AT PHYSIOLOGICAL RATES IN SMOOTH BUT NOT IN FAST-TWITCH SKELETAL MUSCLE. J.W.Walker\*, A.V.Somlyo#, Y.E.Goldman#, A.P.Somlyo# & D.R. Trentham\*, \*MRC London, U.K. & #U. of PA Sch. of Med., Phila., PA.

The sarcoplasmic reticulum of saponin-skinned muscle fiber bundles from rabbit main pulmonary artery (MPA) and mechanically skinned single fibers from frog semitendinosus was loaded with  $\text{Ca}^{2+}$ . The fibers were then incubated in relaxing solutions containing 1.5 mM free  $\text{Mg}^{2+}$  and isomers (probably P-4 and 5 substituted) of 1-(2-nitrophenyl)ethylinositol 1,4,5-trisphosphate (caged  $\text{InsP}_3$ ) at concentrations ( $5 \mu\text{M}$  and  $750 \mu\text{M}$  total caged  $\text{InsP}_3$ , respectively) that did not induce contractions. On laser pulse photolysis at 347 nm and  $20^\circ\text{C}$ ,  $\text{InsP}_3$  was formed at  $220 \text{s}^{-1}$ . In the case of MPA, following a 0.4 s lag phase,  $0.5 \mu\text{M}$   $\text{InsP}_3$  induced a contraction equivalent to that produced by 10 mM caffeine. The rate of contraction was at least as rapid as that of the normal pharmacomechanical coupling response to norepinephrine in intact (not skinned) preparations.  $80 \mu\text{M}$   $\text{InsP}_3$ , liberated from caged  $\text{InsP}_3$ , induced a full contraction in skeletal muscle, but the time to peak was variable and greater than 10 s at 1.5 mM or  $40 \mu\text{M}$  free  $\text{Mg}^{2+}$ . This time to peak is about 3 orders of magnitude greater than the normal excitation-contraction coupling response to an action potential. Endogenous  $\text{InsP}_3$  phosphatase activity within MPA hydrolyzed  $200 \mu\text{M}$   $\text{InsP}_3$  at  $15\text{--}20 \mu\text{M}\cdot\text{s}^{-1}$  and that within frog muscle at  $<0.5 \mu\text{M}\cdot\text{s}^{-1}$ . We conclude that  $\text{InsP}_3$  induced Ca release is sufficiently fast for the proposed role of  $\text{InsP}_3$  as an intracellular messenger in smooth muscle. Supported by NIH grant HL15835 to the PA Mus. Inst.

**Th-AM-B12** INOSITOL 1,4,5-TRISPHOSPHATE-INDUCED CALCIUM RELEASE FROM THE SARCOPLASMIC RETICULUM AND CONTRACTION IN BARNACLE MUSCLE. Eduardo Rojas, Verónica Nassar and Mario Luxoro, Laboratory of Cell Biology and Genetics, NIH, Bethesda, MD and Laboratory of Cellular Physiology, Faculty of Sciences, University of Chile, Viña del Mar, Chile.

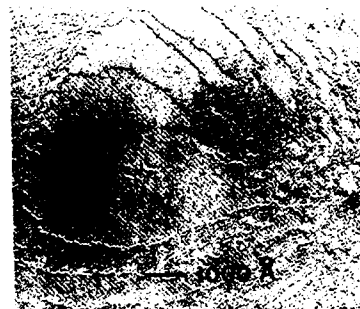
Intracellular applications of a fixed amount of  $\text{InsP}_3$ , from 0.2 to 8 nmol per 50 mg fiber, over brief periods (2 sec) into barnacle muscle fibers induced vigorous contractures. Peak tension attained during the first application depended on  $\text{InsP}_3$  concentration and the maximum tension evoked by the injection of 8 nmol  $\text{InsP}_3$  was  $1.6 \text{ kg/cm}^2$ . Peak tension during the second application of a high dose of  $\text{InsP}_3$  ( $10 \mu\text{M}$ ) was always smaller than that during the first application. Extracellular  $\text{Ca}^{2+}$  could be omitted with no measurable effects on either the amplitude or the time course of the contractures evoked by  $\text{InsP}_3$ . Aequorin was used to measure  $\text{InsP}_3$ -evoked  $\text{Ca}^{2+}$  release from intracellular stores in skinned muscle fibers. Provided the sarcoplasmic reticulum (SR) was pre-loaded with  $\text{Ca}^{2+}$ , application of  $\text{InsP}_3$  in the presence of 1 mM  $\text{Mg}^{2+}$  induced a transient release of  $\text{Ca}^{2+}$  which depended on the concentration of  $\text{InsP}_3$  applied. During each transient,  $\text{Ca}^{2+}$  rose rapidly to a peak value and then returned slowly ( $t_{1/2}$  of 1.5 min) to a basal level. Maximum  $\text{Ca}^{2+}$  release was obtained at a concentration of  $\text{InsP}_3$  below  $100 \mu\text{M}$  and amounted to 4 nmol of  $\text{Ca}^{2+}$  per gram of muscle, enough to increase  $\text{Ca}^{2+}$  from 0.1 to  $8 \mu\text{M}$  had the  $\text{Ca}^{2+}$  release occurred in the intact fiber. These data suggest that as in frog skeletal muscle,  $\text{InsP}_3$  in barnacle muscle may be a second messenger released from the site of  $\text{Ca}^{2+}$  entry at the level of the transverse-tubular membrane which may cause  $\text{Ca}^{2+}$  release from  $\text{Ca}^{2+}$  loaded SR.

**Th-AM-C1** LINEAR AND CYCLIC  $\beta$ -TURNS. G.D. FASMAN AND M. HOLLOSI, Department of Biochemistry, Brandeis University, Waltham, MA 02254.

To find the interrelationship between the chiroptical properties of flexible linear and rigid cyclic models of  $\beta$ -turns, a detailed study on protected linear tetrapeptide (1) and bridged cyclic systems (2) is reported. (1) Z-Gly<sup>1</sup>-X<sup>2</sup>-Y<sup>3</sup>-Gly<sup>4</sup>-OStearyl (Methyl); (2) cyclo[Gly<sup>1</sup>-X<sup>2</sup>-Y<sup>3</sup>-Gly<sup>4</sup>-NH-(CH<sub>2</sub>)<sub>n</sub>-CO], X=Pro, Gly, Ser, Ser(OBu<sup>t</sup>), Y=Pro, Gly, Ser, Ser(OBu<sup>t</sup>), Asp(OBu<sup>t</sup>), Glu(OBu<sup>t</sup>) and Leu, n=2 or 4. While the circular dichroism (CD) of a great majority of the linear models suggests the participation of more than one species in solution, some of these models feature typical class B, C, or D spectra [Woody (1974) in Peptides, Polypeptides & Proteins (Eds. Blout, Bovey, Goodman, Lotan), John Wiley, p. 338-350]. Z-Gly-Gly-Pro-Gly-OSt, with a class C CD spectrum in acetonitrile, was found to assume a dominant type III  $\beta$ -turn conformation in nonpolar solvents. The linear models, Z-Gly-Ser-Y-Gly-OSt [Y=Asp(OBu<sup>t</sup>), Glu(OBu<sup>t</sup>) or Ser(OBu<sup>t</sup>)] show class B spectra with a very strong positive band below 200 nm. Z-Gly-Ser-Ser-(OBu<sup>t</sup>)-Gly-OSt, in dilute chloroform solution, assumes a distorted type II  $\beta$ -turn conformation, held rigid by an extended system of intramolecular H-bonds. The cyclic quasihexapeptides, cyclo[Gly-Ser(OBu<sup>t</sup>)-Ser(OBu<sup>t</sup>)-Gly-NH-(CH<sub>2</sub>)<sub>4</sub>-CO] and cyclo[Gly-Pro-Gly-Gly-NH-(CH<sub>2</sub>)<sub>4</sub>-CO] are characterized by class B spectra in aqueous solution. FT-IR and NMR studies indicate that both models have a type II  $\beta$ -turn conformation, encompassing the Ser-(OBu<sup>t</sup>)-Gly and Pro-Gly sequence, respectively. Finally, the third bridged system, cyclo[Gly-Pro-Ser-(OBu<sup>t</sup>)-Gly-NH-(CH<sub>2</sub>)<sub>4</sub>-CO] showing a class C CD spectrum in H<sub>2</sub>O, adopts a type I  $\beta$ -turn, fixed by 1 + 4 and O<sup>y</sup>...NH intramolecular H-bonds. This is the first class C spectrum reported for a conformationally mobile system in H<sub>2</sub>O. A set of subspectra for  $\beta$ -turns, with reduced band intensities, is suggested for use in the CD analysis of the conformation of polypeptides in solution.

**Th-AM-C2** STUDY OF PROTEIN CRYSTAL GROWTH MECHANISMS BY ELECTRON MICROSCOPY.\* S.D. Durbin, D.E. Palmer and G. Feher, U.C.S.D., La Jolla, CA 92093

Protein crystallization is a poorly understood process. Various indirect methods have been used to study protein crystal growth (1). We report here on a more direct method using electron microscopy to study the mechanisms of growth by observing crystal surfaces. This method is capable of molecular resolution (2), can be applied to crystals of any size, and can potentially be extended to pre-crystalline aggregates for studies of nucleation. Using freeze-fracture and freeze-dry replica techniques, we have observed molecular-height steps on lysozyme crystal surfaces and demonstrated the presence of lattice defects, such as screw dislocations (see Fig.), which may play a role in crystal growth. Work in progress includes the determination of surface changes involved in the cessation of crystal growth.



Electron micrograph of a screw dislocation in a tetragonal lysozyme crystal. Platinum shadowing from below reveals molecular height steps in a spiral pattern. To one side of the dislocation core (arrow) the lattice plane B is a step up (dark step) from plane A, while to the other side B is a step down (light step) from A.

\*Work supported by NIH.

- (1) For review, see G. Feher and Z. Kam (1985) Methods in Enzymology, Vol. 114, pp. 77-112, Academic Press, N. Y.
- (2) L. Bachmann, R. Becker, G. Leupold, M. Barth, R. Guckenberger and W. Baumeister (1985) Ultramicroscopy 16, 305.

**Th-AM-C3** STRUCTURE OF THE GP17 TAIL-FIBER OF BACTERIOPHAGE T7 DETERMINED BY ELECTRON MICROSCOPY, IMAGE PROCESSING, AND SECONDARY STRUCTURE PREDICTION. A.Steven\*, B.Trus<sup>†</sup>, J.Maizel<sup>‡</sup>, M.Unser<sup>¶</sup>, D.Parry\*, J.Wall<sup>§</sup>, J.Hainfeld<sup>§</sup>, W.Studier<sup>§</sup>. \*NIDDK,†DCRT,‡NCI,§VBEIB,§Brookhaven Nat. Lab.

As visualized by negative staining, tail complexes released from purified T7 virions by heat shock consist of a conical tail-tube surrounded by six kinked tail-fibers. The latter are oligomers of the viral protein gp17 (61.5K), and are thought to function by recognizing receptors on susceptible hosts, thereby initiating the infection process. We have derived a molecular model for the tail-fiber by correlating secondary structure predictions based on the known gp17 sequence (Dunn & Studier, J.Mol.Biol.166:477,1985) with information obtained by piece-wise correlation averaging of tail complex images, separately analyzing the core, the proximal half-fiber, and the distal half-fiber. The proximal half-fiber is a uniform rod ~2.5nm wide and 19nm long, which we equate with a domain of ~130 residues up to #280, that has high  $\alpha$ -helical potential and a heptad distribution conducive to the formation of coiled-coils. A linear succession of four globules of total length 19nm forms the distal half-fiber, which we associate with the carboxy-terminal halves (residues #281-553) of the constituent chains. The amino-terminal domains (residues #1-149) are inferred to link the fiber to the tail-tube. This model has been further elaborated by high-resolution scanning transmission electron microscopy of purified fibers. Mass measurements performed on unstained whole fibers (166±23K;SD,N=221) and distal half-fibers(88±10K;N=85) indicate that the fiber is a trimer, consistent with earlier stoichiometry data. In particular, we conclude that the proximal half-fiber is a triple-stranded coiled-coil rope with the participating chains associated in a parallel, 'in register' configuration.

**Th-AM-C4** THE STRUCTURE OF HELICAL POLYMERS OF SICKLE HEMOGLOBIN.

Bridget Carragher, David A. Bluemke, Michael J. Potel and Robert Josephs.  
Department of Molecular Genetics and Cell Biology, University of Chicago, Chicago, Ill.

We have performed three-dimensional reconstructions of helical polymers of sickle hemoglobin using electron micrographs of negatively stained preparations of deoxygenated sickle hemoglobin (HbS). Several classes of helical polymers of varying diameters have been identified, but all appear to be composed of Wishner-Love double strands. Electron micrographs were Fourier filtered prior to reconstruction to increase the signal-to-noise ratio of the images. In addition, piecewise correlation averaging was performed over many helical repeats in order to enhance structural features in the image. Curved particles were straightened by calculating a cubic spline through the curved axis which was then remapped to a straight line. The reconstruction of helical polymers of HbS is complicated by the variability of pitch exhibited by these particles. Most reconstruction algorithms assume the helical twist to be constant and this assumption results in a loss of resolution in the reconstructed image. To improve the resolution of our data we have investigated methods of estimating the instantaneous pitch of the particles based on the cross correlation between particles and model structures of constant pitch. The instantaneous pitch estimated in this manner can be incorporated directly into the reconstruction algorithm, and the estimate can be iteratively refined over several cycles. The determination of the complete three-dimensional structure of the HbS polymers permits an analysis of the molecular interactions between double strands that stabilize the particle.

This work has been supported by NIH grants HL30121(MJP,RJ), HL22654(RJ), and GM07281(DAB).

**Th-AM-C5** COMPUTER-SIMULATED DENSITY MODELING OF SICKLE HEMOGLOBIN POLYMERS

David A. Bluemke, Bridget Carragher, Michael J. Potel and Robert Josephs  
Department of Molecular Genetics and Cell Biology, University of Chicago, Chicago, IL 60637

We have developed a system for modeling density distributions of deoxyhemoglobin S (HbS) polymers for comparison with electron micrographs. The density of each nonhydrogen atom in a molecule was represented as a Gaussian function proportional to the atomic number of the atom. The density of a molecule of HbS was taken to be the sum of the density distributions of the nonhydrogen atoms within the molecule. By locating molecular densities within the HbS unit cell, density projections of crystals were computed by replicating the unit cell along the axes, followed by projection along the appropriate axis. Similarly, density projections of precrystalline helical polymers such as macrofibers and fibers of HbS may be obtained by calculating the 3D repeating unit of the particle from the density distributions of the constituent HbS molecules. The repeating unit is then rotated and translated along the helical axis at a rate determined by the particle pitch. Computed density projections depicting the particle structure may be compared to electron micrographs of negatively-stained preparations of sickle hemoglobin. In this manner, image features may be quantitatively analyzed and related to the molecular arrangement of hemoglobin tetramers. Such computer-simulated models provide a structural approach that is able to link x-ray diffraction data to electron microscopic studies of noncrystalline polymers of HbS.

This work has been supported by NIH grants HL30121(MJP,RJ), HL22654(RJ), and GM07281(DAB).

**Th-AM-C6** A COMPARATIVE STUDY OF UNFOLDED-REFOLDED FORMS OF PHOSPHOGLYCERATE-KINASE ISOLATED FROM TISSUES OF YOUNG AND OLD RATS. Ari Gafni, Kathy Yuh and Alison Zuniga (Intr. by Robert Zand) The University of Michigan, Ann Arbor, Michigan.

Several enzymes have been shown to display modified functional and structural properties when isolated from tissues of old animals as compared with samples of the same enzymes purified from young animals. Thus, the heat inactivation kinetics of phosphoglycerate-kinase (PGK) samples isolated from skeletal or heart muscles of young rats markedly differ from those of the enzyme made from old tissues. A comparative study of the unfolded-refolded forms of these enzymes was undertaken with the aim of critically testing the hypothesis that the age related structural modifications in PGK are purely conformational. To this end samples of PGK purified from tissues of young and old rats were unfolded by 15 hours incubation in a 2 M guanidine: HCl solution at 4°C. In a typical experiment reactivation was achieved by a 10 fold dilution of the unfolded enzyme solutions into a denaturant-free buffer, followed by 4 hours incubation at 25°C. This resulted in a complete restoration of the activity in PGK samples from both young and old muscle. While the extent of reactivation of heart PGK was slightly less than full, it did not depend on the age of the animals. The unfolded-refolded enzymes were subsequently heat inactivated under a variety of experimental conditions. In all experiments we found that the heat inactivation kinetics of the unfolded-refolded "young" and "old" enzymes coincided. Moreover under certain experimental conditions the kinetics were similar to the inactivation pattern of "young" PGK. These results provide strong evidence for the reversibility of age-related effects at the molecular level and support the hypothesis that the modifications induced in PGK in old muscle and cardiac tissue are purely conformational.

**Th-AM-C7** 2-D NMR ANALYSIS OF  $\alpha$ -HELIX INDUCTION IN S-PEPTIDE BY TRIFLUOROETHANOL  
Jeffrey W. Nelson, Dept. of Biochemistry, Louisiana State Univ., Baton Rouge, LA 70808  
Neville R. Kallenbach, Dept. of Biology, Univ. of Pennsylvania, Philadelphia, PA 19104

The  $\alpha$ -helix formed by the S-peptide, residues 1-19 of ribonuclease A, is stabilized by trifluoroethanol (TFE). This stabilization has previously been characterized as a function of pH and temperature by circular dichroism (1), and it was found that the effect of charged groups is not altered by TFE. The TFE titration has now been studied in detail at low pH and temperature, where the helix is most stable, using 2-dimensional NMR techniques to follow the chemical shifts of most of the non-exchangable protons. COSY spectra in D<sub>2</sub>O were predominately utilized, with the help of relay COSY and NOESY spectra in H<sub>2</sub>O to aid in the assignments.

Published NMR studies of the S-peptide in aqueous solution showed that the  $\alpha$ -helix forms from residues 3 to 13, suggesting the presence of a "helix stop signal", which terminates the helix after residue 13 (2). The present studies in TFE indicate that the helix stop signal remains operative in TFE solutions, since between 0 and 20 mole % TFE, only the resonances of residues 3 to 13 show significant changes in their chemical shifts. However, several of the other resonances exhibit small shifts at higher TFE concentrations. This suggests that TFE might stabilize all amino acids, although the residues found to go helical in aqueous solution appear to be stabilized at much lower TFE concentrations. Studies are in progress to attempt to determine quantitatively the effects of TFE on the helix initiation and propagation processes.

- (1) J. W. Nelson and N. R. Kallenbach, *Proteins: Structure, Function and Genetics*, in press.
- (2) P. S. Kim and R. L. Baldwin, *Nature*, 307, 329-334.

**Th-AM-C8** ANALYSIS OF PROTEIN FOLDING USING GEL FILTRATION CHROMATOGRAPHY AT MODERATE PRESSURE.  
Earle Stellwagen, William Shalongo, and M.V. Jagannadham, Department of Biochemistry, University of Iowa, Iowa City, IA 52242.

A number of globular proteins having a single polypeptide chain, ribonuclease, thioredoxin, papain and carbonic anhydrase, were individually injected into a 300 mm Toyo Soda TSK-125 gel filtration column. The column was equilibrated with mobile phase containing isocratic denaturant concentrations at neutral pH at a flow rate of 1 ml/min and a pressure of about 40 bar. The denatured form of each protein elutes about two minutes earlier than its native form, presumably due to the increased effective hydrodynamic volume of the denatured form. The resolution of the native and denatured populations in the denaturation transition zone can be varied from slow to fast exchange by changing the column temperature. The kinetics of the conformational changes of each protein can be observed in the native baseline, transition and denatured baseline zones by independent selection of the denaturant concentrations in the protein sample injected and in the isocratic mobile phase. Observed chromatographic profiles can be simulated for a variety of denaturation mechanisms having adjustable equilibrium and kinetic parameters. Detailed analysis of the chromatographic profiles obtained for thioredoxin indicate that (i) no conformation having an effective volume intermediate between the native and denatured form is populated; (ii) the change in effective volume during refolding is coincident with the change in fluorescence quenching; (iii) a slow folding form is generated in the denatured state; and (iv) a native-like intermediate is transiently populated in the native baseline zone. This investigation was supported by Public Health Service research grants GM22109 and HL14388.

**Th-AM-C9** FLUORESCENCE ANISOTROPY DECAYS INDICATE SHAPE CHANGES IN PHOTO-CROSSLINKED CALMODULIN ON BINDING CALCIUM. Enoch W. Small and Sonia R. Anderson, Department of Biochemistry and Biophysics, Oregon State University, Corvallis, OR 97331 USA.

When bovine brain calmodulin is irradiated with 280 nm light, the two tyrosine residues can react to form bityrosine, a highly fluorescent chromophore with an absorption maximum at 320 nm and an emission at about 400 nm. The affinity of the photo-crosslinked calmodulin for calcium ion is diminished, but the protein apparently retains some native structure because it shows calcium-dependent binding to the proteins myosin light chain kinase and troponin I, and to the peptide mastoparan (Malencik, D. A. & Anderson, S. R., *Biochemistry*, in press). The anisotropy decay of the fluorescence is monoexponential for more than five lifetimes of the fluorescence. Because X-ray crystallographic results of calcium-bound calmodulin indicate a dumbbell-shaped molecule, recovered rotational correlation times are interpreted in terms of such a model. It is concluded that either the transition moment for absorption or that for emission is approximately aligned with the long axis of the dumbbell. The measured 9.9 ns rotational correlation time for the crosslinked calmodulin approximately agrees with the value predicted by the theory using the dimensions of the crystallographic structure. When the temperature is varied from 4.8 to 31.8°C, the recovered correlation times are proportional to the viscosity and inversely proportional to the absolute temperature. Titration of the crosslinked calmodulin from no calcium to high calcium suggests an increase in length of the linkage between the two lobes of the dumbbell.

**Th-AM-C10** EXPOSURE TO LOW pH TRIGGERS REVERSIBLE CONFORMATIONAL CHANGES IN PSEUDOMONAS EXOTOXIN A. Zohreh T. Farahbakhsh, Rae Lynn Baldwin and Bernadine J. Wisnieski. Dept. of Microbiology and the Molecular Biology Institute, University of California, Los Angeles, CA 90024

Exposure to a low pH environment appears to be an obligatory trigger of the Pseudomonas toxin (PTx) entry pathway [J. Biol. Chem. 261, 11404 (1986)]. When we examined the effect of pH upon the conformation of PTx, we found that the intrinsic fluorescence of PTx is strongly dependent on pH, decreasing between pH 7.4 and 4.0 with a red shift in the emission  $\lambda_{max}$ . The changes are reversible and associated with the acquisition of a binding site for the fluorescent dye 1-anilino-8-naphthalenesulfonic acid (ANS). The fluorescence intensity of ANS in the presence of PTx increases with decreasing pH and is accompanied by a blue shift in the emission spectrum, indicative of exposure of hydrophobic surfaces. These changes are also reversible. Both the intrinsic fluorescence and ANS binding profiles show a dramatic dependence on pH, with the transitions centered on pH 5.0 and 4.5, respectively. Circular dichroism studies reveal a 9% decrease in  $\alpha$ -helicity between pH 7.7 and pH 4. The susceptibility of toxin to trypsin cleavage is also a function of pH, increasing with decreasing pH. The pH 7.4 cleavage profile is regained when the acid-treated samples are brought back to pH 7.4. The conformational changes observed in these pH-shift experiments are likely to be physiologically significant because the conditions closely resemble those that the toxin would encounter if entry into the cytoplasm of a cell involves escape from an endosomal compartment. Supported by USPHS GM22240 and the UCLA Academic Senate.

**Th-AM-C11** BPTI IS COMPACT WHEN THE DISULFIDE BONDS ARE REDUCED. D. Amir and E. Haas Dept. Life Sciences, Bar Ilan University, Ramat-Gan, ISRAEL. A series of four BPTI derivatives, labeled with a donor of excitation energy at residue 1 and an acceptor at one of the  $-NH_2$  of lysine residues (15,26,41,46) were prepared. Steady state excitation spectroscopy and fluorescence decay measurements were used to determine interresidue distance distributions. Analysis of donor fluorescence decay curves obtained for all derivatives in the reduced denatured state (in 6M GuHCl) indicates that the protein is not a random coil. Instead, bimodal interresidue distance distribution functions were obtained, indicating the presence of two conformational sub-populations: a compact structure with intramolecular distances similar to those obtained in the native state and an extended conformational sub-population. When the reduced denatured BPTI derivatives are diluted into folding conditions, but kept reduced (no disulfide bonds formed), the measured transfer efficiencies are close to those obtained in the native state for transfer between residue 1 and residues 26,41,46. The transfer efficiency between residues 1 and 15, however, is higher than in the native state (i.e. a shorter distance). These results show that in BPTI, very compact conformations are well populated even under strongly denaturing conditions and that a first step in folding may be a fast collapse into a non-native compact ("molten") globule which is then reorganized into the native oblate conformation, stabilized by the formation of the disulfide bonds and other specific interactions.

**Th-AM-C12** IONIC STRENGTH AND pH DEPENDENCE OF SICKLE HEMOGLOBIN POLYMERIZATION. B.L. GABRIEL, R.J. VASSAR, AND R. JOSEPHS.

The polymerization of deoxygenated suspensions of sickle hemoglobin can proceed through two different pathways that are dependent upon ionic strength and pH. The pathways are referred to as the high pH and low pH pathways, and the characteristic polymeric structures formed in each pathway are different. A "phase diagram" of pH versus ionic strength has been constructed defining the solution conditions governing polymerization. The low pH pathway exists at all values of pH below 6.5 in phosphate buffer at ionic strengths of 20 to 100mM. Above pH 6.5, the high pH pathway occurs at ionic strengths greater than 35mM, and the low pH pathway below ionic strengths of 35mM. The boundary between the two pathways contains a "transition zone" where intermediates of both pathways coexist. The shape of the "phase diagram" suggests that histidine residues play an important role in the polymerization process. This work was supported by NIH Grant HL22654 (R.J.).

**Th-AM-D1 THE FREQUENCY-DEPENDENCE OF THE NMR LONGITUDINAL RELAXATION RATE,  $T_1^{-1}$  OF WATER IN BIOLOGICAL SYSTEMS.**

T.F. Egan, H.E. Rorschach, Rice University, Houston, Texas, and C.F. Hazlewood, Baylor College of Medicine, Houston, Texas.

The NMR spin-lattice relaxation rate,  $T_1^{-1}$ , of bulk water is independent of the Larmor frequency in the normal rf range. However,  $T_1^{-1}$  of intracellular water in biological systems, which accounts for as much as 80% of the cell mass, is frequency-dependent. This indicates that the NMR properties of water in the cellular environment are influenced by long-correlation time processes due to the interaction of water with proteins and other macromolecular constituents of the cell. We have measured the relaxation rate  $T_1^{-1}$  of water in the *Artemia* (brine shrimp) cyst over the proton NMR Larmor frequency range .01 to 500 MHz. The frequency-dependence of  $T_1^{-1}$  is interpreted in terms of a two-phase exchange model. One water phase is similar to pure water and contributes a small constant relaxation rate. The second phase is water closely associated with the surfaces of large molecules. A polymer-dynamics relaxation mechanism, which treats fluctuations of long-chain molecules in aqueous solution, has been proposed to explain the relaxation in this second water phase. In one limit, this mechanism predicts a frequency-dependent relaxation rate proportional to  $\omega^{-2}$ . This particular dependence has previously been observed in other NMR studies on biological systems and is also observed in this study for *Artemia* cysts between 10 and 500 MHz.

<sup>1</sup>H.E. Rorschach and C.F. Hazlewood, *J. Magnetic Resonance*, **69**, 1986.

**Th-AM-D2 PROTON NMR STUDIES OF BACTERIOPHAGE T4 LYSOZYME AIDED BY  $^{15}\text{N}$  AND  $^{13}\text{C}$  ISOTOPIC LABELING: A STRATEGY FOR STRUCTURAL AND DYNAMIC INVESTIGATIONS OF LARGER PROTEINS**

Lawrence P. McIntosh, David C. Muchmore, and Frederick W. Dahlquist, Inst. of Molecular Biology, University of Oregon, OR 97403; Richard H. Griffey, University of New Mexico School of Medicine, Albuquerque, NM 87131; and Alfred G. Redfield, Dept. of Biochem., Brandeis Univ., Waltham, MA 02254

We have developed a strategy for the resolution and assignment of single proton resonances in proteins of molecular weight up to at least 40kD. This approach is based on  $^{15}\text{N}$  or  $^{13}\text{C}$  labeling of selected residues in a protein. Resonances from protons directly bonded to the labeled atoms are detected in two-dimensional (2D)  $^1\text{H}$  vs  $^{15}\text{N}$  or  $^{13}\text{C}$  "forbidden echo" (multiple quantum) spectra. The nuclear Overhauser effects from or to isotopically tagged protons are selectively observed in 1D isotope-directed or -detected NOE (IDNOE) spectra or in 2D isotope-directed NOESY spectra. Using this approach, we have resolved ca. 160 resonances from  $^{15}\text{N}$ -bonded protons in the backbone and side-chains of uniformly  $^{15}\text{N}$ -labeled T4 lysozyme (18.7kD). Partial  $^1\text{H}/^2\text{H}$  exchange is used to simplify the  $^1\text{H}$ - $^{15}\text{N}$  spectrum of this protein. These resonances are identified by amino acid class through selective incorporation of  $^{15}\text{N}$ -labeled amino acids, and are assigned to specific residues by mutational substitution, multiple  $^{15}\text{N}$  and  $^{13}\text{C}$  labeling, and IDNOE measurements. Using these techniques, we are studying the structure and dynamics of wild type and temperature sensitive T4 lysozymes. Amide and indole hydrogen exchange is monitored with 2D  $^1\text{H}$ - $^{15}\text{N}$  spectroscopy and the local structure and motions of selected regions in these proteins are probed by isotope selected relaxation and IDNOE measurements. This strategy is applicable to larger proteins of known sequence and can be used to investigate structure, structural changes, and dynamics in a site-specific manner.

**Th-AM-D3 SOLVENT DEPENDENCE OF  $^1\text{H}$  NUCLEAR OVERHAUSER ENHANCEMENTS AS A TEST OF CONFORMATIONAL RIGIDITY IN BLOOD GROUP "A" and "H" OLIGOSACCHARIDES.**

C. Allen Bush, Zhen-Yi Yan and B. N. Narasinga Rao Dept. of Chemistry, Illinois Institute of Technology, Chicago, IL 60616 U.S.A.

NMR and circular dichroism results in aqueous solution as well as conformational calculations have suggested that the non-reducing terminal sugar residues of blood group oligosaccharides adopt single, well defined conformations which are determined mainly by non-bonded interactions. As a test of the hypothesis that electrostatic, hydrogen bonding and hydrophobic effects do not play a decisive role in determining the conformation of the blood group oligosaccharides, we have studied the  $^1\text{H}$  NMR spectra of a blood group A tetrasaccharide and an H-hexasaccharide in DMSO and pyridine solutions. The proton NMR spectra were assigned by COSY and phase sensitive 2D-HOHAHA techniques and, n.O.e.'s were measured by 1D-difference spectroscopy. As in the aqueous solutions, the strong dependence of the rotational correlation time ( $\tau_c$ ) on temperature enabled observation of either negative n.O.e. at low temperature or positive effects at high temperature or both. The temperature independence of the ratio of n.O.e. between protons held at fixed distances by the pyranoside ring to n.O.e. between those on different residues implies that the conformation is not strongly temperature dependent. The observed n.O.e. are qualitatively similar to those previously reported in  $\text{D}_2\text{O}$  solution. Comparison of n.O.e. calculated as a function of glycosidic dihedral angles showed that a single molecular conformation was consistent with experimental data on the oligosaccharides. The conformations of the oligosaccharides in DMSO solution are essentially identical to those in  $\text{D}_2\text{O}$  and conformations in pyridine are very similar.

Research supported by NIH grant GM 31449 and by NSF grant DMB 85-17421

**Th-AM-D4**  $^{13}\text{C}$ -NMR OF CLOSTRIDIUM PASTEURIANUM FERREDOXIN AFTER REDUCTIVE METHYLATION OF THE AMINES USING  $^{13}\text{C}$ -FORMALDEHYDE. M.R. Gluck and W.V. Sweeney, Department of Chemistry, Hunter College, CUNY, N.Y., NY 10021

Clostridium pasteurianum 2(4Fe-4S) ferredoxin exhibits a pH dependent midpoint reduction potential at pH values greater than 7.0. The pH dependence arises from a reduction-linked proton binding. This ferredoxin contains only two amines, Lys<sup>3</sup> and the N-terminal alanine. The possible contribution of these two amine sites to the observed reduction-linked proton binding was investigated. Reductive methylation of the Ala<sup>1</sup> and Lys<sup>3</sup> amino groups was accomplished using  $^{13}\text{CH}_2\text{O}$  and  $\text{NaCNBH}_3$ . Methylation of the apoprotein or the reduced form of the protein results in nearly complete methylation whereas modification of the oxidized form of the protein results in only about 15% methylation.  $^{13}\text{C}$  NMR spectroscopy was used to titrate the modified amines to determine their pKa values. The pKa of the  $\epsilon, \epsilon'$ -dimethylated Lys<sup>3</sup> amino group remains essentially unchanged with pKa values of 10.4 and 10.2 for the apoprotein and the oxidized form of the protein, respectively. In contrast, the pKa of the  $\alpha$ -amino group of Ala<sup>1</sup> changes considerably, from 6.7 in the apoprotein to 9.5 in the oxidized form of the protein. These results are consistent with the presence of a strong ion pair in the oxidized form of the protein. When the protein is reduced using a hydrogen/hydrogenase system in the presence of methyl viologen, the pKa of the Lys<sup>3</sup> amino group is 10.4 and for Ala<sup>1</sup> the pKa is 9.5. These pKa values are essentially unchanged from the oxidized form of the protein. These results tentatively rule out the amino groups as direct participants in the observed reduction-linked proton binding of this protein.

**Th-AM-D5** INVESTIGATION OF DNA BINDING PROTEINS BY  $^{15}\text{N}$  NMR SPECTROSCOPY:  $\lambda$  CRO REPRESSOR AND THE COMPLEX FORMED WITH OPERATOR AND NON-SPECIFIC FRAGMENTS. Philip Leighton, Michael J. Bogusky, Robert A. Schiksnis, Stanley J. Opella and Ponzy Lu. Department of Chemistry, University of Pennsylvania, Philadelphia, PA 19104.

Uniformly  $^{15}\text{N}$  labelled cro repressor from the bacteriophage  $\lambda$  has been prepared by expression of its gene in Escherichia coli and subsequent growth on a medium containing 98% enriched  $^{15}\text{N}$  ammonium sulfate as sole nitrogen source. Specific residue types were labelled in a similar manner by providing labelled amino acids to the culture. Two-dimensional  $^1\text{H}$ - $^{15}\text{N}$  correlated spectroscopy shows that almost all of the backbone amides and a large number of the side chain nitrogens may be resolved, and that several assignments are possible.

One dimensional NMR experiments are used to measure the heteronuclear NOE.  $^1\text{H}$ - $^{15}\text{N}$  NOE's are sensitive to the mobility of the site on a nanosecond timescale, and hence we are able to observe the changes in dynamics of individual residues of the protein on binding DNA (either non-specific fragments or the specific binding site). These results are compared to those anticipated from the proposed model of cro-DNA interaction.

This research was funded by grants from: The Lindemann Trust, NATO, and NIH.

**Th-AM-D6** MEMBRANE-METHEMOGLOBIN INTERACTIONS STUDIED BY PHOSPHORUS NMR. K. Butler, R. Deslauriers & Ian C.P. Smith, Division of Biological Sciences, National Research Council of Canada, Ottawa, Ontario, Canada K1A 0R6.

Cell lysis and the presence of methemoglobin are both observed in malaria. The interaction of different forms of hemoglobin has been reported to influence the structure and lipid dynamics of membranes. To investigate the possible connection between the presence of methemoglobin and cell lysis in malarial infections, we have studied membranes of phosphatidylethanolamine (PE) and phosphatidylcholine (PC) by  $^{31}\text{P}$  NMR, with a Bruker CXP-300, using CSA echoes and by calorimetry, using a Microcal MC-1. PC:PE (2:1) mixtures were hydrated with 10 mM Tris, or with buffer plus methemoglobin (2:1 protein:lipid). The spectra were the same width, and both showed resolution of the component subspectra. The temperature of the phase transition of DMPE:DMPC 1:1, measured by NMR or by DSC, was not influenced by methemoglobin. Although methemoglobin did not change the gel-liquid crystal transition temperature of DLPE, at 40°C, the relaxation time  $T_1$  decreased from 0.8 sec to 0.3 sec and  $T_2$  decreased from 1.5 to 1.0 msec. Methemoglobin and heme raised the midpoint of the bilayer-hexagonal phase transition of egg PE. These compounds and native hemoglobin caused the appearance of an isotropic peak at 50°C, that remained on cooling but disappeared after freezing and thawing. Erythrocyte ghosts and the extracted lipids gave typical bilayer patterns that were not perturbed by methemoglobin. Subspectra were not resolved, possibly due to the heterogeneity of the lipid. We conclude that methemoglobin-lipid interaction stabilizes the lamellar phase of the lipids, and therefore is not involved in the red cell fragility observed in malaria.



**Th-AM-D7 STUDY OF CATARACT AND ITS PREVENTION WITH AN ALDOSE REDUCTASE INHIBITOR IN DIABETIC RATS BY P-31 NMR SPECTROSCOPY.** P. Mahendroo, D. Thomas, M. Lou and R. Garadi;  
Conner Research Center, Alcon Laboratories, Inc., Fort Worth, Tx. 76134.

Cataract is one of the secondary complications of diabetes mellitus. Early stages of diabetic cataract are characterized by appearance of vacuoles, followed by opacification of the lens nucleus and finally the entire lens. The initiating molecular mechanism of this type of cataract, usually called sugar cataract, is abnormal polyol pathway activity. High plasma glucose concentration in diabetics apparently results in high lens glucose concentration. This excess glucose is converted to its sugar alcohol, sorbitol, by the enzyme aldose reductase. The intracellular accumulation of these sugar alcohols produces a hyperosmotic effect that results in cellular swelling. As the swelling progresses lenticular parameters start changing and, if left unchecked, results in water clefts and vacuoles. We have used P-31 NMR spectroscopy to study prevention of cataract in experimental diabetic rats by the most potent aldose reductase inhibitor, AL1576, (Spiro-(2,7-difluorofluorene-9, 4'imidazolidine)-2,'5'-dione) using high energy phosphorus metabolites as the molecular probe. In order to understand effect of diabetes on lens ATP, and cell membrane marker phosphorylcholine, we carried out a two week and an eight week diabetic rat (streptozotocin induced) P-31 NMR studies. In the two month untreated group, lenses became cataractous accompanied by drastic depletion of ATP and PC. In the group treated by the ARI, AL1576, the clarity of lenses is maintained and both ATP & PC levels remain in the normal range. For the first time we have quantified the devastating effect of diabetes on lens P-31 metabolites by non-invasive NMR spectroscopy. The results of these studies will be discussed.

**Th-AM-D8 PROTON NMR STUDY OF ISCHEMIC RAT HEARTS: ROLE OF DESFERRIOXAMINE.** Jin-Shan Wang, Sandra Z. DeRolf and Hara P. Misra. (Intr. by Dr. Germille Colmano.) Department of Biosciences, College of Veterinary Medicine, Virginia Tech, Blacksburg, VA 24061

NMR techniques do provide information about myocardial metabolism. Proton NMR spectroscopy seems especially interesting since it can be used to monitor some chemical moieties that are characteristically altered and vary in relation to the severity of myocardial ischemia.

We have observed release of lactic acid from the myocardium of isolated rat hearts subjected to ischemia and reperfusion. H-1 spectra were obtained at 200 MHz and 270 MHz with a Bruker NMR instrument. Two groups of peaks corresponding to DL-lactic acid sodium salt ( $C_3H_5NaO_3$ ) were observed in the H-1 spectra. The doublet observed at 1.3 ppm corresponds to  $CH_3$  and the quartet observed at 4.1 ppm is from group CH. They are coupled with a coupling constant of 6.8 Hz. Desferrioxamine ( $10^{-4}$  M), an iron chelator, was found to inhibit the release of lactic acid. This suggests that the release of lactic acid during reperfusion of hypoxic heart tissue is mediated by either an iron-catalyzed reactive intermediate or by an activated iron complex.

**Th-AM-D9  $^{23}Na$  AND  $^{39}K$  NMR VISIBILITY IN RAT HEARTS.** A. Dutta, J.A. Balschi, J.S. Ingwall, T.W. Smith, & C.S. Springer, NMR Laboratory, Harvard Medical School, Boston, MA 02115; Dept. of Chemistry, SUNY Stony Brook, NY 11794-3400.

The use of shift reagents (SR) in the study of  $^{23}Na$  and  $^{39}K$  NMR spectra of intact hearts allows for the possibility of making transport measurements *in vivo*. However, the degree of NMR visibility ( $v$ ) of the signals from these cations in the various cardiac compartments must be ascertained in order to fully exploit this approach. Hearts were excised from male Sprague-Dawley rats and perfused in the Langendorff mode, with K-H buffer solution at 37° C in order to wash away all the blood, till they achieved normal performance. They were removed from the cannula, dropped into an NMR tube with 3 mL isotonic mannitol solution, and a high-resolution spectrum was obtained. The hearts were then homogenized and dissolved with Acationox and a strong base, and an NMR spectrum obtained of the homogenate. With the use of calibration standards, the overall heart [Na] and [K] were determined from the homogenate spectrum. These were found to be 54 mM and 57 mM, respectively. From literature compartmental volumes (V) and accepted values for the compartmental [Na] and [K], the expected overall [Na] and [K] are 58 mM and 62 mM, respectively. However, for both  $^{23}Na$  and  $^{39}K$ , the peak area from the homogenate spectrum was 2.5 times that from the intact heart. This yields an overall  $v$  of 0.4 for each cation in the intact heart. Interestingly, this is the value expected from dynamic and/or static quadrupolar effects anticipated for these  $I = 3/2$  nuclei in tissue if the entire spectrum is excited but only the  $1/2$  to  $-1/2$  transition is observed. These results appear to be incompatible with our  $^{23}Na$  and  $^{39}K$  NMR spectra of intact beating hearts perfused with SR (Biophys. J. 48:159 (1985)). In these, the peak assigned to  $Na_i$  accounts for ca. 1% of the total  $^{23}Na$  spectral area and that to  $K_i$  for 64% of the  $^{39}K$  signal observed. The contributions expected from the  $Na_i$  and  $K_i$  are ca. 7% and ca. 97%, respectively. Among the possible reasons for this discrepancy are: (a) errors in curve resolution and integration of the SR-perfused heart spectra; (b) entry of SR into some intracellular spaces; (c) different values for  $v_i$  and  $v_o$ ; (d) inaccurate literature values for  $[Na_i]$ ,  $[K_i]$ ,  $V_i$  and/or  $V_o$ ; and (e) inhomogeneous distributions of cations in the intracellular spaces (among various organelles).

**Th-AM-D10 SUBSTRATE REGULATION OF THE NUCLEOTIDE POOL DURING ISCHEMIA AND REPERFUSION IN ISOLATED HEART PREPARATIONS: A P-31 NMR ANALYSIS**

S.A. Camacho, W. Parmley, S. Wu, T.L. James, R. Sievers, E. Botvinick and J. Wikman-Coffelt. Cardiovascular Research Institute and Department of Pharmaceutical Chemistry, University of California, San Francisco.

The factors which influence myocardial recovery from ischemic insults are not well understood. We studied the effect of glucose (GLU) vs pyruvate (PYR) as the sole energy substrates during ischemia and reperfusion in Langendorff rat heart preparations. Using P-31 NMR spectroscopy, baseline high-energy phosphate levels (ATP, PCr, Pi) and intracellular pH (pHi) were compared with values during 30 min. of left coronary artery ligation (LIG) followed by 30 min. of reperfusion (REPER). Reversible occlusion was confirmed by: 1) adding Coomassie blue dye to the perfusate thereby outlining the ischemic zone, 2) measuring the reduction in wall thickness during LIG with two-dimensional echocardiography and 3) measuring the drop in oxygen consumption and total coronary flow during LIG and documenting a return toward baseline with REPER. GLU perfused hearts had a greater decrease in pHi during LIG ( $7.07 \pm 0.01$  to  $6.36 \pm 0.10$ ), than PYR perfused hearts ( $7.06 \pm 0.02$  to  $6.83 \pm 0.04$ ). REPER resulted in rapid return to baseline pHi values in both groups. During LIG, ATP values decreased a greater amount in GLU vs PYR hearts ( $57 \pm 4\%$  and  $79 \pm 5\%$  of baseline respectively). REPER did not significantly change ATP levels in either GLU or PYR perfused hearts. PCr/Pi ratio was reduced to  $9 \pm 2\%$  and  $10 \pm 2\%$  of baseline in GLU and PYR perfused hearts respectively during LIG. REPER resulted in partial recovery of PCr/Pi ratio to  $40 \pm 5\%$  and  $37 \pm 5\%$  of baseline for GLU and PYR groups respectively. Coronary effluent inosine and hypoxanthine losses as measured by HPLC were over two times greater during both LIG and REPER in GLU perfused hearts. We conclude that perfusion with PYR, which bypasses rate-limiting glycolysis, decreases intracellular acidity during LIG. This leads to reduced nucleotide washout which allows more rapid ATP resynthesis resulting in higher ATP levels.

**Th-AM-D11 EVIDENCE FOR VOLATILE ANESTHETICS BINDING TO HEMOGLOBIN IN INTACT ERYTHROCYTES.**

David Y.-E. Li and Alice M. Wyrwicz, Department of Chemistry, University of Illinois at Chicago, Chicago, IL 60680

$^{19}\text{F}$  NMR spectroscopy has been used to study the interaction between volatile anesthetics, halothane and methoxyflurane, with intact erythrocytes. Our results indicate that these compounds easily penetrate the cell membrane and bind reversibly to hemoglobin within the cell. Binding to the membrane lipids is negligible in the intact cells. The  $^{19}\text{F}$  spin-lattice relaxation time measurements also indicate binding to hemoglobin and corroborate the chemical shifts results. These findings were confirmed with studies on lysed red blood cells, isolated hemoglobin and membrane fragments (ghosts). Both anesthetics have a finite and distinct number of sites on hemoglobin, accessible to them in the intact cells. The same behavior is observed *in vivo* as well as *in vitro*. Environmental variations in the binding sites, as indicated by  $^{19}\text{F}$  chemical shifts, have been observed among the several mammalian erythrocytes studied. The most pronounced difference has been observed between rabbit and human hemoglobin, most likely resulting from the amino acid(s) substitution in the binding pocket.

Supported by NIH grants GM29520, GM33415 and RCDA K04GM00503 to AMW.

**Th-AM-D12 ULTRASOUND INDUCED INCREASE IN MYOCARDIAL CONTRACTILITY: METABOLIC EFFECTS MEASURED BY P31 MR SPECTROSCOPY.** George V. Forester, Y. Geoffrion, O. Z. Roy & I. C. P. Smith (Intr. by S. Jacobson). Division of Electrical Engineering and Division of Biological Sciences, National Research Council of Canada, Ottawa, Canada K1A 0R6.

We have shown that ultrasound application (1 W/cm<sup>2</sup> SATA at 1 MHz) to myocardium results in an increase in contractility. This has been tested in isolated papillary muscle, Langendorff perfused preparations and *in situ* with anesthetized animals. However, the sequence of biological events which leads to the beneficial effect has not been elucidated. An examination of the metabolism of the heart during ultrasound exposure should help in solving this problem. We built a high resolution NMR probe which would allow simultaneous perfusion of an isolated rat heart, pacing, measurement of  $^{31}\text{P}$  metabolites, heart mechanical activity and application of ultrasound.

During normoxic perfusion, ultrasound increased rate pressure product (the contractility index), [CrP] remained constant, as did the Pi/CrP. However under hypoxia, [CrP] decreased and Pi/CrP increased. Ultrasound application increased the contractility index, reducing the [CrP] and increasing Pi/CrP. Under hypoxia, when the heart was paced to 300/min, [CrP] decreased more and Pi/CrP increased. Ultrasound application increased the contractility and further increased the Pi/CrP while reducing [CrP]. These preliminary data suggest that ultrasound increases contractility by augmenting the Cr-CrP shuttle; under normoxic conditions the shuttle is not activated by the ultra-sound, but under hypoxic conditions and with pacing, when the supply demand ratio shifts to the demand side, the shuttle is activated and further pushed by the application of the ultrasound. When ultrasound application is stopped, the metabolic effects including the augmentation of contractility are reversed.

**Th-AM-E1** EFFECT OF POSITION OF CHARGES AND  $\alpha$ -HELICAL POTENTIAL ON LIPID ASSOCIATION AND LECITHIN:CHOLESTEROL ACYL TRANSFERASE ACTIVITY OF THE AMPHIPATHIC HELIX.

G.M. Anantharamaiah, A. Gawish, M. Igbal, Kiran Gupta, R.M. Eband, Intr. by Jere P. Segrest: Department of Pathology of Medicine, University of Alabama at Birmingham and Department of Biochemistry, McMaster University, Ontario, Canada.

Based on the theory of the amphipathic helix, which has been proposed to explain the lipid-associating properties of exchangeable plasma apolipoproteins, four peptides have been synthesised and studied. These peptides have been designed to increase the alpha-helix forming probability, in a model peptide which does not associate with dimyristoylphosphatidyl choline. Similar changes were made on a moderately lipid associating peptide. The resulting peptide analogs and the complexes formed with DMPC were studied by using negative stain electron microscopy, circular dichroism, intrinsic tryptophan fluorescence, and differential scanning calorimetry techniques. The four analogs,  $[E^{4,9}_{L^{11,17}}]$  reverse-18A,  $[E^{4,9}_{L^{5,11,17}}]$  reverse-18A,  $[E^{1,8}_{L^{11,17}}]$  18A, and  $[E^{1,8}_{L^{5,11,17}}]$  18A were derived from a model amphipathic peptide; Asp-Trp-Leu-Lys-Ala-Phe-Trp-Asp-Lys-Val-Ala-Glu-Lys-Leu-Lys-Glu-Ala-Phe (18A) whose lipid binding properties strongly mimic apolipoprotein A-I and has been studied in detail (3). Although the modified analogs had comparable lipid associating activity, modified 18A peptide analogs were superior in their ability to activate the enzyme lecithin:cholesterol acyl transferase (LCAT) compared to modified reverse-18A analogs indicating that the positions of charged residues in the amphipathic helix plays an important role in LCAT activation.

**Th-AM-E2** BILAYER PERTURBATIONS INDUCED BY SIMPLE HYDROPHOBIC PEPTIDES. Russell E. Jacobs & Stephen H. White, Dept. of Physiology and Biophysics, University of California, Irvine, CA 92717

The interactions peptides of the form Ala -X-Ala -O-R (n=1,3; R=methyl, t-butyl) with DMPC bilayers have been examined using NMR spectroscopy. Tripeptides with X = Ala, Leu, Phe, and Trp incorporated into acyl chain perdeuterated DMPC bilayers have been examined. A tripeptide with X = uniformly deuterated Ala has been examined incorporated into bilayers and as a polycrystalline powder. Lipid  $^2H$  NMR spectra show that the addition of peptide disorders the bilayer and that the extent of the perturbation increases as the size of the central residue increases. Moment analyses of the spectra indicate that, while the average acyl chain order parameter decreases with increasing central residue size, the order parameter spread across the bilayer increases. Lipid segmental  $^1H$  spin-lattice relaxation rates,  $1/T_1(i)$ , exhibit a square-law functional dependence on  $S_{CD}(i)$  both with and without the addition of peptide. The addition of peptide causes an increase in the slope of plots of  $1/T_1(i)$  versus  $S_{CD}(i)^2$  with little change in the  $1/T_1(i)$  intercept. Within the context of theories of spin-lattice relaxation in membranes, these results imply that the peptides have a large influence on slow, probably long-range collective motions, while not significantly affecting fast local lipid motions.  $^2H$  NMR spectra of deuterated peptide in DMPC bilayers have both isotropic and powder pattern components which vary as a function of temperature. Preliminary 2D-NOE experiments using members of the heptapeptide series indicate the presence of specific lipid-peptide interactions. The implication of this data for determining the location of the peptides in the bilayer will be discussed. Research supported by NSF, NIH, and the AHA-Calif. Affiliate.

**Th-AM-E3** CONFORMATION AND ORIENTATION OF GRAMICIDIN A IN ORIENTED PHOSPHOLIPID BILAYERS MEASURED BY SOLID STATE CARBON-13 NMR. Bruce Cornell, and Frances Separovic, Commonwealth Scientific Industrial Research Organisation, Australia, P.O.Box 52 North Ryde N.S.W. 2113, Australia, and Ross Smith and Attilio J. Baldossi, University of Queensland, St Lucia, Queensland 4067, Australia. Four analogues of the helical ionophore gramicidin A have been synthesised with carbon-13 labelled carbonyls incorporated at either Gly<sup>2</sup>, Ala<sup>3</sup> or Val<sup>7</sup>. A fourth compound incorporated  $^{13}C$  at both the carbonyl and  $\alpha$ -carbon of Gly<sup>2</sup> within the same molecule. These labels were studied using solid state, proton enhanced,  $^{13}C$  nuclear magnetic resonance (NMR) in hydrated dispersions of dimyristoylphosphatidylcholine (DMPC)-gramicidin A. The dispersions were aligned on glass cover slips whose orientation to the magnetic field could be varied through  $180^\circ$ . The orientation dependence of the NMR spectrum was used to obtain an accurate measurement of the  $^{13}C$  chemical shift anisotropy (CSA) and in the case of the fourth compound, the  $^{13}C$ - $^{13}C$  dipolar coupling constant. From the measured CSA and estimates of the orientation of the  $^{13}C$  shielding tensor, we are able to determine the direction of the  $^{13}C=O$  bonds and to compare these with the predictions of the various reported models for the configuration of gramicidin A in phospholipid bilayers. Our results are consistent with the left-handed  $\pi\pi^{6.3}_{LD}$  single stranded helix (Urry, et al., 1982. J. Membrane Biol., 69, 225-231). The right-handed  $\pi\pi^{6.3}_{LD}$  single-stranded helix observed for gramicidin A in sodium dodecyl sulphate micelles (Arseniev, et al., 1985. FEBS Lett., 186 168-174) yields a poorer fit to the data.

**Th-AM-E4** STUDIES ON THE CONSENSUS AMPHIPATHIC HELICAL DOMAINS OF APOLIPOPROTEINS A-I AND A-IV. Jere P. Segrest, Ali Gawish, M. Iqbal, Kiran Gupta, and G.M. Anantharamaiah: Department of Pathology, Biochemistry and Medicine, University of Alabama at Birmingham, Birmingham, Alabama.

The amphipathic helix has been generally presumed to be the structural form of lipid-associating domains of apolipoproteins A-I and A-IV. Cloning and sequencing studies of apolipoproteins have suggested that a primordial 11mer amino acid sequence was duplicated to produce tandem repetitive 22mer amphipathic helical domains in apo A-I and A-IV. Amino acid consensus sequences for apo A-I and apo A-IV, and an analog of apo A-I with a neutral residue at the non-polar face instead of negatively charged residue, have been synthesized and studied. All these peptides have a comparable  $\alpha$ -helicity in aqueous buffer as studied by circular dichroism (27<sup>o</sup>o, 36<sup>o</sup>o, and 32<sup>o</sup>o for apo A-I, [Ala 12] apo A-I and apo A-IV consensus, respectively). However, they differ in their lipid associating properties. Studies of these synthetic peptides have been initiated to provide insight into the structural and functional differences in apolipoproteins A-I and A-IV. The apo A-IV analog and the alanine analog of the apo A-I consensus interact instantly to clarify the multilamellar vesicles of dimyristoyl phosphatidyl choline to form small discoidal complexes (Stokes diam 62±20Å and 75±12Å respectively). The apo A-I consensus interacts slowly and the discoidal complexes formed at the same peptide:lipid weight ratio are larger (>200Å). These results indicate that the presence of a negatively charged residue at the nonpolar face drastically reduces its lipid-associating ability. The lipid-association of apo A-I probably comes from the cooperativity of the amphipathic helical domains; the charged residue on the nonpolar face in 5 out of 9 tandem repetitive domains may have biological significance.

**Th-AM-E5** FOURIER TRANSFORM INFRARED STUDIES OF THE INTERACTION OF CaATPase WITH BINARY MIXTURES OF PHOSPHOLIPIDS. Richard Mendelsohn and Markian S. Jaworsky, Dept. of Chemistry, Rutgers University, 73 Warren Street, Newark, NJ, 07102.

FT-IR and DSC have been used to monitor the tendency of CaATPase to partition into regions of chemical structure and physical order in complex lipid environments. The IR experiment involves the use of acyl-chain perdeuterated phospholipids as one component of a reconstituted ternary complex of two lipids plus protein. This approach enables simultaneous examination of the order and melting characteristics of each phospholipid using the configuration-sensitive acyl chain C-H (C-D) stretching frequencies of the proteated (deuterated) species.

Unusual partitioning behavior was observed in complexes of DEPC/DMPC-d<sub>54</sub> and DEPC/DPPE-d<sub>62</sub>. In the former system, composition-dependent protein-induced effects on lipid melting properties were noticed. At low levels of DEPC, gel phase domains of this species are present, from which CaATPase is excluded. At high levels of DEPC, both components have their melting processes broadened and shifted to lower temperatures, suggesting that protein interacts in similar fashion with both lipids. In the latter system, CaATPase selects a fixed phospholipid composition for its immediate environment, independent of the initial lipid composition in the reconstitution protocol. The CaATPase thermal denaturation follows the sequence (mostly  $\alpha$ -helix→antiparallel  $\beta$ -sheet→random coil). The  $\beta$  sheet→random coil interconversion temperature coincides with the gel-liquid crystal transition temperature of domains of relatively pure DPPE-d<sub>62</sub>. No such protein transition is seen for CaATPase in its native lipid environment, although the  $\alpha$  helix→ $\beta$  sheet interconversion is observed.

**Th-AM-E6** PHOSPHOLIPID DOMAINS IN BIOLOGICAL MEMBRANES: A P-31 NMR STUDY

<sup>†</sup>Philip L. Yeagle, Arlene D. Albert, <sup>‡</sup>Barry S. Selinsky, <sup>#</sup>Bruce a. Cornell and <sup>‡</sup>James Frye. <sup>†</sup>Department of Biochemistry, School of Medicine, University of Buffalo, Buffalo, NY 14214, USA; <sup>#</sup>NIH, PO Box 12233, Research Triangle Park, NC 27709; <sup>#</sup>Division of Food Research, CSIRO, North Ryde, NSW, Aus.; <sup>‡</sup>Dept. of Chemistry, Colorado State University, Fort Collins, CO 80523.

P-31 NMR studies on several biological and reconstituted membranes have produced spectra containing at least two distinct spectral components. Multiple powder patterns have been observed in P-31 NMR spectra from biological membranes containing cytochrome oxidase, calcium pump protein, and rhodopsin. We have now obtained P-31 NMR spectra suitable for lineshape analysis in three reconstituted systems; one containing human erythrocyte and a third containing sarcoplasmic reticulum calcium pump protein. In these systems the two spectral components can be simulated by axially symmetric powder patterns. One powder pattern is the same as observed for the pure lipid in the absence of the protein. The other powder pattern is more than twice as broad. Spectral simulations show excellent agreement between the model and the observed spectra. Resimulations of all of the above data show quantitative agreement among the data from several laboratories. Modulation of domain sizes is described. A new model for the protein-induced formation of these domains is described that encompasses the population of the domain, the measured rate of exchange between the domains in the membrane and the structure of the membrane proteins involved.

**Th-AM-E7 PSEUDO-CAPACITANCE OF BILAYER ALAMETHICIN INTERACTION.**

Igor Vodyanoy, James E. Hall, and Vitaly Vodyanoy. Department of Physiology and Biophysics, University of California, Irvine, Irvine, CA 92717.

It has been shown that alamethicin and its derivatives alter membrane voltage-dependent capacitance (Biophys.J. 47, 254a, 1985). This effect depends on both concentration and charge of alamethicin. Our experimental data can be explained in terms of a potential-dependent pseudo-capacitance associated with adsorbed alamethicin. Pseudo-capacitance is expressed as a function of alamethicin charge, its concentration in the bathing solution and the applied electric field. The theory well describes the nonmonotonic dependence of the capacitance on applied voltage and alamethicin concentration. It describes the decrease of the voltage-dependent capacitance when potential is positive at the bilayer side where negatively charged alamethicin is added and the lack of change of the voltage-dependent capacitance at negative potentials. Positively charged alamethicin, on another hand, will increase the voltage-dependent capacitance if added to the bilayer side where negative potential is applied and will not change the voltage-dependent capacitance if potential is positive. When alamethicin is neutral the theory predicts no change of the voltage-dependent capacitance at any sign of applied voltage. Experimental data are consistent with the model in which alamethicin molecules interact with each other while being adsorbed to the membrane surface. The energy of this interaction depends on the alamethicin concentration. Supported by grants from NIH GM 30657, NSF BNS-8508495, and US Army grants DAAG29-85-K-0109 and DAAL03-86-G-0131.

**Th-AM-E8 <sup>13</sup>C NMR STUDIES OF OLEIC ACID INTERACTIONS WITH HEPATIC FATTY ACID BINDING PROTEIN.**

David P. Cistola, Mary T. Walsh, Ronald P. Corey, James A. Hamilton and Peter Brecher.

Biophysics Institute, Boston University School of Medicine, Boston, MA 02118.

<sup>13</sup>C NMR spectroscopy was used to probe the structural interactions between carboxyl <sup>13</sup>C-enriched oleic acid (18:1) and cytosolic fatty acid binding protein (FABP) from rat liver. At pH 8.6, <sup>13</sup>C NMR spectra of systems containing 2-8 moles 18:1 per mole FABP exhibited only one 18:1 carboxyl resonance. The chemical shift value for this resonance (182.2 ppm) was substantially different from that for protein-free 18:1 samples under identical conditions (181.1 ppm) but similar to values for several resonances corresponding to 18:1 bound to bovine albumin (182.0-182.3 ppm; J.S. Parks, D.P. Cistola, D.M. Small, D.M. & J.A. Hamilton, 1983, J. Biol. Chem. 258:9262). Hence, the observed resonance most likely corresponded to 18:1 bound to FABP. Between pH 7.0 and 5.1, the bound resonance exhibited a partial ionization shift with an estimated apparent pK (<5) similar to monomeric carboxylic acids in water in the absence of protein. This ionization behavior suggested that the carboxyl groups of bound 18:1 molecules were anionic (at pH >6.5), solvent-accessible, and not involved in electrostatic interactions with cationic residues of FABP. At pH <7.5, 18:1/FABP samples became visibly turbid, and a second carboxyl resonance (180.4 ppm at pH 7.5) was observed. This broad upfield resonance was similar to the resonance obtained for protein-free samples of 18:1 at pH <7.5, and most likely represents unbound self-associated lamellar aggregates of 18:1. We conclude: (i) the carboxyl(ate) group of 18:1 bound to FABP experiences only one type of binding environment; (ii) the 18:1/FABP binding interaction is not electrostatic, but most likely hydrophobic; (iii) 18:1 partitions between protein-bound and unbound (lamellar) pools at pH values <8.0.

**Th-AM-E9 PARTITIONING OF OLEIC ACID BETWEEN HEPATIC FATTY ACID BINDING PROTEIN AND PHOSPHOLIPID VESICLES.** David P. Cistola, Ronald P. Corey, Peter Brecher and James A. Hamilton.

Biophysics Institute, Boston University School of Medicine, Boston, MA 02118.

<sup>13</sup>C NMR spectroscopy was used to monitor the partitioning of carboxyl <sup>13</sup>C-enriched oleic acid (18:1) between rat liver fatty acid binding protein (FABP) and sonicated egg phosphatidylcholine vesicles (PC). <sup>13</sup>C NMR spectra of systems containing equal concentrations (w/v) of FABP and PC and from 1 to 4 moles of total fatty acid (FA) per mole FABP exhibited two 18:1 carboxyl resonances (182.2 ppm and 178.5 ppm) at pH 7.4. The upfield peak (178.5 ppm) corresponded to 18:1 bound to PC vesicles at pH 7.4 (Hamilton, J.A. and Cistola, D.P., 1986, Proc. Natl. Acad. Sci. 83, 82), and the downfield peak corresponded to 18:1 bound to FABP. At 1/1 mole ratio (FA/FABP), the intensities of both peaks were approximately equal. However, with increasing 18:1 content, the intensity of the PC-associated 18:1 peak increased relative to that for the FABP-associated peak. Since the spin-lattice relaxation time (T<sub>1</sub>) and nuclear Overhauser enhancement (NOE) were identical for both peaks (T<sub>1</sub>=0.5 sec; NOE=1.3), the relative peak intensities reflected relative mole content of FABP- and PC-bound 18:1. Hence, in the system containing a total of 4 moles FA per mole FABP at pH 7.4, 1 mole 18:1 was bound to each mole of FABP and the remaining 3 moles 18:1 was bound to PC. The partitioning of 18:1 between FABP and PC changed only slightly with changing pH between pH 8.5 and 5.5. We conclude that 18:1 partitions between FABP-bound and membrane-bound pools at physiologic pH and favors membrane binding with increasing 18:1 content. Like extracellular albumin, intracellular FABP may function *in vivo* to solubilize and transport FA. However, unlike albumin, FABP may not function to prevent FA from accumulating in cellular membranes.

**Th-AM-E10** CHARACTERIZATION BY FRAPP AND QELS OF REVERSE MICELLAR SOLUTIONS UPON MYELIN PROTEOLIPID UPTAKE. D.Chatenay., W.Urbach. Laboratoire de Physique. Ecole Normale Supérieure, 24 rue Lhomond 75005 Paris, France. C.Nicot., M.Vacher., M.Waks. ER 64-01 CNRS. 45 rue des Saints Pères 75006 Paris, France.

One of the most hydrophobic integral membrane proteins, the Folch-Pi proteolipid from bovine brain (50% of total myelin proteins) can be inserted into the aqueous core of reverse micelles constituted of sodium bis (2-ethylhexyl) sulfosuccinate (AOT) in hydrocarbon solvents. The solubilization of this protein-lipid complex in an assembly of membrane-mimetic character requires : (i) the presence of a definite amount of interfacial water (  $[H_2O] / [AOT] = 7$  ) (ii) the binding of at least 5 molecules of positively charged myelin phospholipids per 30,000 dalton protein as characterized by HPLC. (iii) a relatively high concentration of AOT (300 mM). Failure to fulfill all the above experimental conditions leads to the proteolipid insolubility. These results suggest the involvement of more than one micelle per molecule of myelin protein in the solubilization process. Structural studies of proteolipid-free and proteolipid-containing micellar solutions carried out at several AOT concentrations by two complementary techniques, fluorescence recovery after fringe pattern photobleaching (FRAPP) and quasi elastic light scattering (QELS), indicate the formation of structures which are compared to those described by Ramakrishnan et al (*J.Biol.Chem.* 1983. 25, 4857) for rhodopsin in lipid complexes.

**Th-AM-F1 CHLORIDE CONDUCTANCE OF HUMAN RED BLOOD CELLS AT VARIED  $E_K$ .** Jeffrey C. Freedman and Terri S. Novak, Dept. of Physiology, SUNY Health Science Ctr. at Syracuse, Syracuse, NY 13210.

Net K and Cl effluxes induced by the K ionophore valinomycin (VAL) or by cation-selective gramicidin (GRAM) channels have been determined at varied external K, or  $K_o$ , in the presence and absence of the anion transport inhibitors DIDS and SITS. Fresh washed human red blood cells were suspended at 1.2 % hematocrit in media containing x mM KCl, 150-x mM NaCl (for VAL) or 150-x mM choline Cl (for GRAM), and 5 mM HEPES buffer, pH 7.4 at 23°C. KCl efflux was initiated by addition of 1  $\mu$ M VAL or 60 nM GRAM, and triplicate samples were analyzed for K and Cl before and 10 min after addition of the ionophore. The results indicate that pretreatment with 10  $\mu$ M DIDS or 100  $\mu$ M SITS for 30 min only partially inhibits Cl conductance at 1 mM  $K_o$ . However, as  $K_o$  is increased such that  $E_K$  approaches the normal resting potential, inhibition by DIDS becomes virtually complete. For example, with VAL the percent inhibition by DIDS increased from 59  $\pm$  11% at 1 mM  $K_o$  to 87  $\pm$  8% at 60 mM  $K_o$  (SD,n=6). With GRAM, inhibition increased from 67  $\pm$  2% to 87  $\pm$  10% (SD,n=4). The partial inhibition by DIDS at 1 mM  $K_o$  was maximal and was not increased by increasing (DIDS), temperature, or the time of exposure to DIDS. Controls indicated that cell shrinkage was not responsible for the partial inhibition by DIDS at 1 mM  $K_o$ . The same pattern of DIDS inhibition was seen in the presence of the optical potentiometric indicator WW781. Parallel flux and voltage measurements suggest that human red blood cell chloride conductance at near-normal resting potentials is completely DIDS-sensitive, and by inference entirely mediated by capnophorin; a second DIDS-insensitive pathway becomes appreciable at hyperpolarizing potentials below about -40 mV. Supported by NIGMS grant GM28839.

**Th-AM-F2 SODIUM PHOSPHATE COTRANSPORT IN HUMAN ERYTHROCYTES.** D. G. Shoemaker, C. A. Bender, and R. B. Gunn. Dept. of Physiology, Emory Univ. School of Medicine, Atlanta, GA 30322.

Influx of inorganic phosphate, [ $^{32}$ P] $_o$  = 1 mM, into erythrocytes was examined at 37°C in a high (140 mM) sodium ( $Na^+$ ), 10 mM HEPES-buffered (7.4) medium at 37°C. Cells are shown to transport  $P_i$  by a 4,4'-dinitrostilbene-2,2'-disulfonate (DNDS) -sensitive pathway (70%), a sodium-dependent pathway (25%), and a pathway linearly dependent on phosphate concentration up to 2.0 mM  $P_i$  (5%). Kinetic evaluation of this  $Na^+$ ,  $P_i$  cotransport pathway determined the  $K_i$  for activation by  $Na^+$  ( $[Na^+]_o$  = 1.0 mM) and  $P_i$  ( $[P_i]_o$  = 140 mM) to be 139  $\pm$  4 mM and 304  $\pm$  24  $\mu$ M, respectively. The sodium ( $^{22}Na$ ) influx ( $\pm P_i$ ) and the  $P_i$  influx ( $\pm Na^+$ ) was measured in the presence of 0.2 mM DNDS, 0.1 mM ouabain, 0.1 mM bumetanide, and 1.0 mM amiloride at three extracellular pH values (6.90, 7.40, 7.75). Phosphate-independent sodium influx ( $\leq 25 \mu$ M  $P_i$ ) was constant at 3.30 mmoles (Kg Hb) $^{-1}$  (hr) $^{-1}$  at both pH 6.90 and 7.40, being elevated to 4.01  $\pm$  0.16 at pH 7.75. Conversely the sodium-independent ( $\leq 0.5$  mM  $Na^+$ )  $P_i$  influx was constant at 0.075 mmoles (Kg Hb) $^{-1}$  (hr) $^{-1}$  at 7.40 and 7.75 being increased to 0.34  $\pm$  0.02 at pH 6.90. Despite the asymmetric behavior of the co-ion-independent influxes the  $Na^+$ ,  $P_i$  cotransport was not significantly different at the three pH values examined. Phosphate-dependent sodium influx increased from 0.66 to 0.79 as the pH was raised from 6.90 to 7.40 while the sodium-dependent phosphate influx increased from 0.38 to 0.46, thereby maintaining a constant  $Na^+$ : $P_i$  stoichiometry of 1.7:1.0. Hill coefficients for sodium activation of  $P_i$  transport give values not significantly different from 1.0. These data are consistent with a model of  $Na^+$ ,  $P_i$  cotransport involving two sodium sites of differing affinities (10 and 140 mM). (Supported by AHA, Georgia Affiliate (DGS) and NIH grant HL 28674 (RBG).)

**Th-AM-F3 CHOLESTEROL MODULATION OF TRANSPORT PROCESSES IN AGE FRACTIONATED RED BLOOD CELLS.** M.A. Zanner, T.R. Sisneros, and W.R. Galey. Dept. of Physiology, University of New Mexico School of Medicine, Albuquerque, New Mexico 87131.

Previous studies by our laboratory have shown that band 3 mediated anion exchange is increased in older circulating human RBCs (Zanner and Galey, 1985). In addition, we have shown that the osmotic water permeability of aged RBC membranes is also increased (Sisneros, et al, 1985). Other investigators have reported that young and old red blood cells differ in cholesterol content (Pranker, 1958; Cohen et al, 1976; Shiga et al, 1979; Bartosz, 1981). Studies by Sha'afi et al, (1969) have shown that the osmotic water permeability of the RBC membrane appears to be independent of membrane cholesterol content, and Grunze et al, (1980) have reported that cholesterol enrichment of red cells inhibits  $SO_4^{-2}$  self exchange whereas cholesterol depletion enhances  $SO_4^{-2}$  transfer. These observations have led us to investigate the possibility that cholesterol may be responsible for the changes in transport which we have observed in age-separated cells.

Human red cells were separated by density (and age) according to the technique of Murphy (1973). Young and old RBCs were cholesterol depleted and enriched using the techniques of Grunze et al. Our results indicate that a 50% depletion of cholesterol in young RBCs leads to a significant increase in anion transport of 25% and also an increase in water permeability of 20%. Cholesterol enrichment of old RBCs leads to a decrease in anion transport of 20% and a lesser decrease in water permeability of 5%. This data leaves open the possibility that cholesterol content may be responsible for transport differences in young and old red cells.

**Th-AM-F4** IDENTIFICATION OF A PROTEIN EXTRACTED FROM THE MEMBRANES OF HUMAN RED CELLS WHICH IS ASSOCIATED WITH CA-DEPENDENT INHIBITION OF THE Na,K ATPase. D.R. Yingst, D.M. Polasek, G. Sheiknejad; Dept. of Physiology, Wayne State University, School of Medicine, Detroit, MI 48201

An extract of human red blood cells prepared at low ionic strength in the presence of EDTA was previously shown to increase Ca-dependent inhibition of the Na,K ATPase and has now been purified by means of Ca-dependent hydrophobic interaction chromatography. The most purified sample contains two proteins as observed by SDS PAGE under reducing conditions: one of approximately 35,000 daltons and calmodulin of 18,000 daltons. The addition of fractions containing these two proteins (at an estimated total protein concentration of 77 ng/ml) increased Ca-dependent inhibition of the Na,K ATPase from less than 20% to more than 45% at 2  $\mu$ M free Ca. The original extract tested at a final concentration of 213,000 ng/ml only increased the inhibition to 35%. Of the total purified protein added to the assay 7 ng/ml or 0.2 nM was contributed by the 35,000 dalton protein (giving a ratio of 4 molecules per Na,K pump) and 70 ng/ml or 4 nM was due to the calmodulin. The addition of purified calmodulin alone at a final concentration of 5 nM had no effect, indicating that either the 35,000 dalton protein or the combination of the 35,000 dalton protein and calmodulin caused the increased inhibition. The 35,000 dalton protein may be calnaktin, a soluble protein proposed to increase Ca-dependent inhibition of the Na,K ATPase. The amount of the 35,000 dalton protein extracted from the membrane is in the range of 100 to 300  $\mu$ g per liter cells which would be approximately 0.5 to 1.5 molecules per Na,K pump. (Supported by NIH: GM 3223-3 and AM 01253-03, a RCDA to DRY).

**Th-AM-F5** EFFECTS OF TRANSPORT SITE CONFORMATION AND ANION BINDING ON THE AFFINITY OF THE HUMAN RED BLOOD CELL ANION TRANSPORT PROTEIN FOR NIFLUMIC ACID (NA). P. A. Knauf, N. A. Mann, and L. J. Spinelli. Dept. of Biophysics, Univ. of Rochester Med. Ctr., Rochester, NY 14642

The red cell anion exchange protein (band 3) can exist in two different conformations, one (E<sub>i</sub>) in which the transport site can bind cytoplasmic (inside) anions and another (E<sub>o</sub>) in which it can bind anions in the external medium. There are also forms in which anions (X<sup>-</sup>) such as Cl<sup>-</sup>, I<sup>-</sup> or SO<sub>4</sub><sup>=</sup> are bound to form the corresponding EX<sub>i</sub> and EX<sub>o</sub> complexes. To determine whether or not these different forms of band 3 differ in their affinity for the noncompetitive inhibitor, NA, we have measured NA inhibition of Cl<sup>-</sup> exchange at 0°C and have determined the dissociation constants for NA from the intersection points of Dixon plot (1/J versus NA) lines as follows:

Form	Lines with different	at constant	NA diss. const.	Mean	S.D.
E <sub>o</sub>	Cl <sub>o</sub>	Cl <sub>i</sub>	K <sub>e</sub>	0.19 $\mu$ M	0.04
E <sub>io</sub>	I <sub>o</sub>	Cl <sub>o</sub> , Cl <sub>i</sub>	K <sub>f</sub> (I)	0.30 $\mu$ M	0.05
ES <sub>o4o</sub>	SO <sub>4o</sub>	Cl <sub>o</sub> , Cl <sub>i</sub>	K <sub>f</sub> (SO <sub>4</sub> )	1.40 $\mu$ M	0.16
E <sub>i</sub>	Cl <sub>i</sub>	Cl <sub>o</sub>	K <sub>g</sub>	0.66 $\mu$ M	0.02
E <sub>ii</sub>	I <sub>i</sub>	Cl <sub>o</sub> , Cl <sub>i</sub>	K <sub>h</sub> (I)	1.57 $\mu$ M	0.14

These data confirm previous qualitative observations that NA binds preferentially to the E<sub>o</sub> conformation. They further show that I<sup>-</sup> and SO<sub>4</sub><sup>=</sup> binding reduce the affinity for NA, and suggest that the decrease in affinity may be related to the size and/or charge of the substrate. These data also show that NA can be used to alter the conformational distribution of the protein and that the inhibitory potency of NA can provide information about the "native" conformational distribution of the band 3 protein. (Supported by NIH Grant AM 27495 and Fogarty Fellowship TW 00975.)

**Th-AM-F6** BAND 3 IS THE BINDING SITE FOR NEUTRAL OR NEGATIVELY CHARGED MACROMOLECULES. TL Fabry and ZG Zhang. Division of Gastroenterology, Department of Medicine, Mt. Sinai School of Medicine, City University of New York, New York. (Intr. by ME Fabry)

Erythrocyte aggregation and sedimentation involves the binding of neutral or negatively charged macromolecules to the erythrocyte membrane. In order to determine whether the binding site for the macromolecules is Band 3, the chloride-bicarbonate transport protein of the erythrocyte membrane, we demonstrated that (a) known inhibitors of the transport protein decrease aggregation and (b) macromolecules known to promote aggregation inhibit the chloride-bicarbonate exchange. We showed that the extent of aggregation is decreased by the reversible inhibitors ASA and DNDS (acetylsalicylic acid and 4,4'-dinitro-2,2'-stilbene disulfonate) of the chloride bicarbonate antiporter and is completely inhibited by DIDS (4,4'-diisothiocyanato-2,2'-stilbene disulfonate), an irreversible inhibitor. This inhibition is independent of the nature of the macromolecule leading to aggregation: we observed it both for fibrinogen and dextran. If the mechanism of the inhibition for aggregation is due to binding to the transport site, then neutral or negatively charged macromolecules should inhibit chloride-bicarbonate exchange across the erythrocyte membrane. We measured the inhibition of the chloride-bicarbonate exchange over a range of bicarbonate concentrations by a dextran (average molecular weight 17,500), which is too short to cause aggregation but should bind to the membrane by the same mechanism as longer polymers. Dextran was a competitive inhibitor with an inhibitor constant, K<sub>i</sub> of 9.8 mM at 25°C.



**Th-AM-F7** EXPRESSION OF BAND 3 IN XENOPUS LAEVIS OOCYTES MICROINJECTED WITH IN VITRO PREPARED mRNA. A.M. Garcia, R. Kopito and H.F. Lodish. Whitehead Institute, Nine Cambridge Center, Cambridge, MA 02142.

Band 3, the anion transporter from red blood cells, has been cloned in our laboratory (Kopito and Lodish, Nature, 316: 234-8, 1985). We have prepared in vitro mRNAs coding for the complete band 3 molecule as well as for a mutant in which the first 1340 nucleotides, coding for the cytoplasmic domain, have been deleted. These mRNAs have been microinjected into *Xenopus laevis* oocytes. Immunoprecipitation of oocytes microinjected with mRNA coding for total band 3 show a single polypeptide of MW 95 kD. These oocytes show an increase in  $^{36}\text{Cl}$  influx when compared with mock injected oocytes. The  $\text{Cl}^-$  transport is DIDS sensitive and bumetanide insensitive, thus showing band 3-like properties. In contrast, oocytes that have been microinjected with mRNA coding for the membrane spanning domain show three polypeptides of apparent MW 45, 50 and 55 kD which are precipitated by antibodies against band 3.  $^{36}\text{Cl}$  influx into these oocytes is lower than into oocytes expressing the whole band 3 molecule. We are currently investigating the reasons for this lower transport capacity. Also, using site directed mutagenesis we are trying to identify the DIDS binding site.

This research was supported by grants from the Cystic Fibrosis Foundation (FO41 7-01) and the National Institutes of Health (AM/GM 37571).

**Th-AM-F8** KINETIC EFFECTS OF INTERNAL AND EXTERNAL PROTONS ON Na/Na EXCHANGE OF RABBIT RED CELLS (RBC). Kevin Morgan and Mitzy Canessa. Dept. of Medicine, Harvard Medical School, Brigham and Women's Hospital, Boston, MA 02115.

We report here the interactions of  $\text{H}^+$  at the internal and external Na sites of the Na/Na exchanger which can promote Na/H exchange. RBC containing variable cell  $\text{Na}(\text{Na}_i$  3 to 92 mM) and pH ( $\text{pH}_i$  6 to 7.4) were prepared by nystatin and DIDS treatment for measurements of initial rates of  $^{22}\text{Na}$  efflux into K and Na media ( $\Delta = \text{Na}/\text{Na}$  exchange). At  $\text{pH}_o$  7.4 the  $K_m$  for  $\text{Na}_i$  to stimulate Na efflux into K media was 60 mM and the  $V_{\text{max}}$  was 12 mmol/l cell  $\times$  h (FU). At  $\text{pH}_o = \text{pH}_i$  7.4, Na/Na exchange has a  $K_m$  for  $\text{Na}_i$  of 18 mM and a  $V_{\text{max}}$  of 12 FU indicating that  $\text{Na}_o$  (150 mM) modifies the affinity for  $\text{Na}_i$ . At  $\text{pH}_o$  7.4,  $\text{Na}_i$  25 and  $\text{Na}_o$  150 mM, an increase in  $\text{H}_i$  ( $\text{pH}_i = 6.5$ ) stimulated Na/Na exchange ( $V_{\text{max}}$  55 FU) and Na/H exchange ( $\text{H}^+$  efflux and Na influx). Furthermore, at acid  $\text{pH}_i$  (6.5) the activation by  $\text{Na}_i$  became sigmoidal (Hill coefficient 2.6) and the  $K_m$  for  $\text{Na}_i$  increased to 68 mM indicating that Na/Na exchange is competitively inhibited by  $\text{H}_i$  at low  $\text{Na}_i$  but stimulated at high  $\text{Na}_i$ .

At  $\text{pH}_i = \text{pH}_o$  7.4,  $\text{Na}_i$  26 mM, the dependence of Na/Na exchange on  $\text{Na}_o$  reveals high ( $K_m$  6 mM) and low ( $K_m$  117 mM) affinity sites with  $V_{\text{max}}$  of 2.5 and 12 FU respectively. Varying  $\text{pH}_o$  ( $\text{pH}_i$  7.3,  $\text{Na}_i$  26 mM) inhibited Na/Na exchange with a  $\text{pK}$  6.4. At  $\text{pH}_o$  6.5, the  $K_m$  of the high and low affinity sites increased and the  $V_{\text{max}}$  of each component did not change suggesting that  $\text{H}_o$  are competitive inhibitors at both external Na sites.

We conclude that  $\text{H}_i$  interact with at least two  $\text{Na}_i$  sites of the Na/Na exchanger;  $\text{H}_i$  cis inhibition of a high affinity  $\text{Na}_i$  site at low  $\text{Na}_i$  can promote Na/H exchange whilst  $\text{H}_i$  stimulation at high  $\text{Na}_i$  promotes Na/Na exchange.  $\text{H}_o$  cis inhibited  $\text{Na}_o$  sites of Na/Na and Na/H exchange.

**Th-AM-F9** KINETIC EFFECTS OF INTERNAL AND EXTERNAL  $\text{H}^+$  ON Li/H AND Li/Na EXCHANGE OF HUMAN RED CELLS (RBC). Mitzy Canessa and Anda Spalvins. Endocrine-Hypertension Unit, Brigham and Women's Hospital and Harvard Medical School, Boston, Ma 02115.

To define if Li/Na exchange can be operated by a Na/H exchanger, we have investigated the kinetic effects of  $\text{H}^+$  on Li and Na transport. RBC containing only K and K+Li (15 mM) were prepared by nystatin and DIDS treatment to vary cell pH between 8 and 5.8. At  $\text{Li}_o$  and  $\text{Na}_o = 150$  mM, net Li and Na influx (mmol/l  $\times$  h = FU) into K cells increased in a sigmoidal fashion ( $n = 2.5$ ) when  $\text{pH}_i$  fell below 7 at  $\text{pH}_o$  8 but not at  $\text{pH}_o$  6.  $\text{H}_i$  stimulated more Na/H ( $V_{\text{max}} = 30 \pm 12$  FU,  $n = 6$ ) than Li/H ( $V_{\text{max}} = 16 \pm .8$  FU,  $n = 3$ ) exchange. The  $K_m$  for  $\text{H}_i$  to stimulate Li influx was higher (560 nM) than for Na influx (354 nM). At  $\text{pH}_i$  6.8, the  $K_m$  for  $\text{Li}_o$  to stimulate Li influx increased from 10 to 50 mM when  $\text{pH}_o$  decreased from 8 to 6, without a change in  $V_{\text{max}}$ , indicating that  $\text{H}_o$  was a competitive inhibitor. The  $K_m$  for Na (50 mM) to stimulate Na/H exchange was higher than for  $\text{Li}_o$  to stimulate Li/H exchange, a property that can account for its 10 times lower  $\text{IC}_{50}$  for amiloride inhibition. The lower rate of Li/H than Na/H exchange can be accounted by a tighter binding of Li requiring higher  $\text{H}_i$  to promote the off reaction of Li entry.

At constant  $\text{pH}_o$  8, Li/Na exchange (140 mM  $\text{Na}_o$ ) was stimulated by a fall in  $\text{pH}_i$  below 7.2 with a  $\text{pK}$  6.8 and inhibited only below  $\text{pH}_i$  6, in agreement with the lower  $K_m$  for  $\text{Li}_i$ . At constant  $\text{pH}_i$  6.5 the dependence of Li/Na exchange on  $\text{pH}_o$  indicated the presence of an inhibitory site with  $\text{pK}$  6.8.

We conclude that Li/Na exchange can be operated by a Na/H exchanger. Both transport modes have lower rate of Li than Na transport and they are subjected to the asymmetrical kinetic effects of  $\text{H}^+$  with affinities for  $\text{H}^+ \text{Li} \gg \text{Na}$ .

**Th-AM-F10** CHANGES IN THE PROTEIN PROFILE OF RAT ERYTHROCYTE MEMBRANES PRODUCED BY TWO MYOTONIA-INDUCERS: CLOFIBRATE AND ANTHRACENE-9-CARBOXYLIC ACID.

A. Morales-Aguilera, Z. Jiménez-Salas, A. Sampayo-Reyes. División de Farmacología Unidad de Investigación Biomédica del Noreste, IMSS. Apdo. Postal 020-E, 64720, Monterrey, Nuevo León. MEXICO.

The protein profile of rat erythrocyte membranes was determined after long-term exposure of the animals to three myotonia-inducers: 20,25-diazacholesterol (20,25-D), clofibrate, and anthracene-9-carboxylic acid (9-AC). Four groups of five Sprague-Dawley male rats each were used; one for control and one for each drug. Drugs were administered daily by means of esophageal cannula at the following doses: 20,25-D ( $50 \text{ mg}\cdot\text{kg}^{-1}$ ), clofibrate ( $300 \text{ mg}\cdot\text{kg}^{-1}$ ) and 9-AC ( $32 \text{ mg}\cdot\text{kg}^{-1}$ ). The control group received only propylenglycol (which was the vehicle) at the same volume than the other groups ( $\sim 0.2 \text{ ml}$ ). After 40 days of treatment, blood was extracted by cardiac puncture under pentothal anesthesia. Erythrocyte membranes were obtained as described by Atkinson *et al.* (1980). After homogenization of the membranes, electrophoresis in discontinuous gels of SDS-polyacrilamide (5% and 8%; Laemmli, 1970) was performed. 20,25-D did not produce any detectable change in the protein profile, as was expected after Chalikian and Barchi (1982) results with sarcolemma, but clofibrate significantly diminished Band 2 density and 9-AC produced the almost complete disappearance of a band similar to that described as Band 7 in human erythrocytes by Goodman & Schiffer (1983).

**Th-AM-G1** DIFFERENTIAL POLARIZATION IMAGING OF TRANSCRIPTIONALLY ACTIVE AND INACTIVE NUCLEOLI, MICKOLS, WM., MAESTRE, M.F., DEPT. OF CHEM. UNIV. OF CAL. BERKELEY, LAWRENCE BERKELEY LABORATORY

We have developed a scanning-stage differential polarization microscope and studied the maturation of live primary spermatocytes of *Drosophila melanogaster*. We used linear and circular differential extinction to give images dependent on the long range order within the nuclei. No staining is required; in fact, as the images are mainly caused by scattering of light, there is minimum light absorption to damage the cells. The scanning stage differential polarization microscope consists of a monochromatic light source (430 nm) whose polarization is sinusoidally modulated by a photoelastic modulator. The light passes through 100X UV polarization retaining objectives and is focused onto a photomultiplier tube. The photomultiplier tube output signal contains primarily circular differential extinction at the polarization modulation and primarily linear differential extinction at twice that frequency. Each frequency has a different sensitivity to linear and circular differential effects. These are calibrated using a polarizer as a linear dichroism standard and different CD standards for different wavelengths. With this information the linear and circular differential extinctions are separated (Rev. Sci. Inst. 56, 1985 p 2228). This information is recorded as the object is scanned across the light beam. The differential images of the transcriptionally active early growth stage of the primary spermatocyte is characterized by different structures in the center vs. the exterior of the nucleolus as well as other structures which are probably the lampbrush chromosomes. The late growth stage of the primary spermatocyte shows a two domain nucleolus with no other obvious structures within the nuclei. Thus, polarization-dependent images reveal ordered structures which correlate with the transcriptional activity of the cell.

**Th-AM-G2** STRUCTURAL FEATURES OF DNA OLIGONUCLEOTIDES CONTAINING MISMATCHES AND C·G BASE PAIRS. S.K. Wolk, F.H. Arnold\*, P. Cruz†, G.T. Walker, I. Tinoco, Jr., Dept. of Chemistry, University of California, Berkeley, CA 94720, \*Dept. of Chemical Engineering, California Inst. of Technology, †Dept. of Biological Chemistry, Wright State University, Dayton, Ohio, 45435

The solution conformations of the self-complementary DNA oligonucleotides dCCCGGG, dCCCAGGG, and dCCCTGGG have been studied by circular dichroism (CD) and nuclear magnetic resonance (NMR) spectroscopy. dCCCGGG forms a perfectly paired duplex, while dCCCAGGG and dCCCTGGG form duplexes with one mismatch, A·A and T·T, respectively. Chemical shift of the aromatic protons of the mismatch bases vs. temperature indicate that these bases are stacked within the helix. One and two dimensional Nuclear Overhauser Effect experiments (1D-NOE and 2D-NOESY) support this conclusion. 2D-NOESY crosspeaks between the aromatic protons and the 2' and 3' sugar protons are consistent with the sugars being in a predominantly southern (2' endo) conformation, as is consistent with standard B form geometry. In seeming contrast, the CD spectra of all three oligonucleotides appear similar to that of the A form polymer poly(rG)·poly(rC). The #1' resonances for several guanosine residues appear as a pseudo-triplet with  $J(1'-2') + J(1'-2'')$  equal to 14 Hz. Thus, CD and NMR data together suggest that these structures have neither classical A form nor B form geometry. They must be in rapid exchange between these forms, or in some intermediate structure.

**Th-AM-G3** LIGATION AND FLEXIBILITY OF 3-ARM AND 4-ARM NUCLEIC ACID BRANCHED JUNCTIONS. \*Mary L. Petrillo, \*Colin J. Newton, \*Richard D. Sheardy, \*Nadrian C. Seeman, †Rong-Ine Ma and †Neville R. Kallenbach, \*Dept. of Biology, SUNY/Albany, NY 12222, Dept. of Chemistry, †Pennsylvania State Univ., Hazleton, PA 18201, and †Dept. of Biology, Univ. of Pennsylvania, Philadelphia, PA 19104.

Nucleic acid branched junctions are stable analogs of structures involved in the process of recombination. The way in which they fulfill their biological function is dependent upon their conformational flexibility. One way to estimate the flexibility of nucleic acid junctions is to ligate them together and to observe which closed products are obtained. We have done this with three different 3-arm junctions, two in which the junction is flanked by three Watson-Crick base pairs and one in which the junction is flanked by two Watson-Crick base pairs and a G-G pair. We have also performed the experiment with a 4-arm junction. In all cases the junctions are separated by 20 nucleotide pairs. All expected short linear products, starting with dimers, were observed for all ligations. All ligations involving adjacent arms resulted in a macrocyclic series which began with trimers. Thus, over the time of the reactions, the arms of both types of junctions were able to form angles as low as 60°. This indicates a larger amount of flexural, and perhaps torsional, flexibility than previously believed for these structures.

This research has been supported by grants ES-00117, GM-29554 and Ca-24101 from the NIH.

**Th-AM-G4** NMR INVESTIGATION OF UNMODIFIED YEAST tRNA<sup>phe</sup> AND VARIANTS. K. B. Hall\*, J. Sampson†, A. Redfield\*, O. Uhlenbeck†, and J. Abelson‡. \*Department of Biochemistry and Physics, Brandeis University; †Department of Chemistry, University of Colorado, Boulder; ‡Department of Biology, California Institute of Technology.

Using T4 RNA polymerase, we have synthesized NMR quantities (about 10 mg) of several yeast tRNA<sup>phe</sup> sequences. These include the wild-type, and the wild-type with the 19 nucleotide intron in the anti-codon. All tRNAs are unmodified (e.g., no methyls or dihydrouridines). Using NMR, we are observing the structure and dynamics of these tRNAs to attempt to relate their structure to their activity in aminoacylation. Because there are no modifications, the NMR spectra do not closely resemble the normal (*in vivo*) tRNA, so the first task has been to partially identify resonances: the acceptor stem and a portion of the D-stem have been identified by a combination of 1-D NOE walks down the helices and NOESY. From a comparison of the chemical shifts, the presence of the intron does not perturb the tRNA acceptor stem. Temperature studies indicate a selective stabilization of some resonances in the presence of the intron; this result remains to be correlated with the biphasic melting of the intron variant.

**Th-AM-G5** ROLE OF EXCITATIONS IN HELIX MELTING, E. W. Prohofsky, Dept. of Physics Purdue University, W. Lafayette, IN 47907

The melting of the helix involves the separation of particular bonds. When viewed from the perspective of excitations this implies that particular excitations can play an important role in inducing the melting. We describe a self-consistent calculation which shows the onset of melting in a format that allows the contribution of individual vibrational modes to be determined. We find that the modes associated with interstrand breathing motion are dominant in bringing about the thermal fluctuations needed to induce melting. We have also studied the elongation melting in polydG.polydC about a single melted base pair. In that case bands between 80 and 120 cm<sup>-1</sup> are important at elongation in one direction (3' → 5' in G strand) and another group of bands below 20 cm<sup>-1</sup> are important for elongation in the opposite direction. Another band at  $\approx 70$  cm<sup>-1</sup> dominates the melting of the continuous polymer with no melted defect. The model predicts that in one case the melting is initiated at the minor groove and in the others from the major groove. The predicted melting temperature is  $\approx 70$ C. A phenomenological model of the mechanism for a simple system will be displayed as well as results on the DNA polymer both with and without defect.

**Th-AM-G6** ETHIDIUM BINDING TO LEFT-HANDED Z-RNA INDUCES A COOPERATIVE TRANSITION TO RIGHT-HANDED RNA AT THE INTERCALATION SITE. C. C. Hardin, G. T. Walker and I. Tinoco, Jr., Dept of Chemistry, University of California, Berkeley, CA 94720.

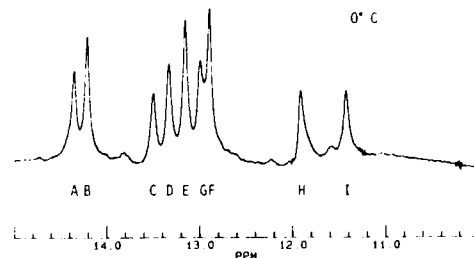
The equilibrium binding of the ethidium cation (Etd<sup>+</sup>) to the right-handed A-form of poly[r(C-G)] and the left-handed Z-forms of both Br-poly[r(C-G)] and Br-poly[d(C-G)] stabilized under physiological conditions was investigated using optical methods. Scatchard analysis indicates that Etd<sup>+</sup> intercalates into poly[r(C-G)] (A-RNA) in a non-cooperative manner. Correlations of ethidium absorbance binding isotherms and polynucleotide circular dichroism data are interpreted as indicating that the drug binds to Br-poly[r(C-G)] (Z-RNA) and Br-poly[d(C-G)] (Z-DNA) resulting in cooperative conversion from left-handed (Z) forms to similar right-handed intercalated conformations. Approximate stoichiometries for the left- to right-handed transitions are 1 Etd<sup>+</sup>/11 base pairs for Z-RNA and 1 Etd<sup>+</sup>/9 base pairs for Z-DNA. The equilibrium binding constants (at 22°C and 220mM NaCl) for Etd<sup>+</sup> intercalation into Z-DNA and poly[d(C-G)] (B-DNA) are approximately 3-fold higher than for the respective Z-RNA and A-RNA. Enthalpies obtained by Van't Hoff analysis of absorbance Etd<sup>+</sup> thermal dissociation data for A-RNA and B-DNA are of similar magnitude. Finally, it is shown that Br-poly[r(C-G)] is not recognized by anti-Z-RNA antibodies upon intercalation, consistent with an altered conformation.

**Th-AM-G7** COMPARISON OF PREFERRED SITES OF DNA BINDING BY BIS-(1,10-PHENANTHROLINE) Cu(I) AND THE CARCINOGENS ACETYLACETOXYAMINOFLUORENE AND BENZO(a)PYRENE DIOL EPOXIDE. James M. Veal, Carolyn Waldron, Maura L. Hamrick, and Randolph L. Rill, Dept. of Chemistry and Institute of Molecular Biophysics, Florida State University, Tallahassee, FL 32306.

The bis-(1,10-phenanthroline) Cu(I) complex (CuOP) in the presence of molecular oxygen and a thiol reducing agent causes spontaneous cleavage of DNA strands. Benzo(a)pyrene diol epoxide (BPDE) and acetylacetoxyaminofluorene both form DNA base adducts that are alkali labile. We have used methods analogous to those employed for DNA sequencing to map sites of binding of these three chemicals to cloned, linear DNA fragments of the sea urchin *S. purpuratus* early histone H3 and H2a genes to a resolution at or near the sequence level. All three reagents react preferentially at a limited number of sites. CuOP appears to exhibit the greatest specificity. Most sites of medium to highly preferred CuOP binding are also sites of preferred binding by AAAF or BPDE. Several of these preferred sites are located near the TATAA box and other potential control sequences 5'-flanking the genes. Other preferred sites occur in and near the 3'-mRNA termination sequences which form a hairpin loop in the product mRNA. Since all of these reagents have polycyclic aromatic ring structures and are potential intercalating agents, the similarities in binding specificities may be related to sequence-dependent peculiarities in DNA conformation that provide sites for facile intercalation. (Supported by contract EVO5888 from the Department of Energy.)

**Th-AM-G8** One- and Two-Dimensional NMR Studies of Carcinogen-Nucleic Acid Adducts. The Structure of d(CCAC<sup>AAF</sup>GCACC)·d(GGTGCGTGG). Thomas R. Krugh, David G. Sanford, and Guanjin Huang, Department of Chemistry, University of Rochester, Rochester NY 14627

N-acetoxy-2-acetylaminofluorene was used to chemically modify the oligodeoxynucleotide d(CCACGCACC) to produce the acetylaminofluorene derivative at the C<sub>6</sub> position of the single guanine (d-CCAC<sup>AAF</sup>GCACC). Duplex model systems were formed by mixing this modified oligodeoxynucleotide with the complementary strand d(GGTGCGTGG) in a 1:1 mole ratio. The AAF-modified nonanucleotide duplex was studied by a variety of techniques. <sup>1</sup>H-<sup>1</sup>H NOE experiments show that the majority of the duplex is in a right-handed conformation. One of the guanines adjacent to the site of modification is in a *syn* conformation. The proton spectrum of the duplex recorded at 0°C shows that all 9 imino resonances are observable, ruling out the base-displacement intercalation model. The structure of AAF-modified DNA will be discussed. This work was supported by NCI grant CA-35251 and by NIH grant RR-01317 to Syracuse University.



**Th-AM-G9** NMR ANALYSIS OF THE CHROMOMYCIN-d(ATGCAT) COMPLEX. R.H. Shafer, M.A. Keniry, S.C. Brown and E. Berman, Department of Pharmaceutical Chemistry, School of Pharmacy, University of California, San Francisco, CA 94143 and The Weizmann Institute, 76100 Rehovot, Israel.

The interaction between the sugar-containing antitumor antibiotic chromomycin A3 and the self-complementary hexanucleotide d(ATGCAT) has been studied by 1D and 2D NMR techniques. Addition of the drug to the oligonucleotide leads to an upfield splitting of the G-C imino protons and protection of the interior A-T imino protons from exchange with the solvent. Non-exchangeable protons were assigned by 2D COSY and NOESY experiments. While the effects observed for the imino protons due to complexation with the drug are characteristic of intercalative binding, results obtained for the non-exchangeable protons show that the mode of binding is not intercalation. <sup>31</sup>P NMR studies also show that the interaction is different from both intercalation and minor groove binding. Several NOE contacts of the drug chromophore and sugar protons with DNA aromatic protons indicate that binding occurs in the major groove, which is rare for non-covalent drug-DNA complexes. Intra- and internucleotide NOEs between aromatic and sugar 1' protons reveal that one of the oligonucleotide strands deviates significantly from the standard B conformation. Supported by NIH Grant CA 27343 and Grant 84-00011 from the US-Israel Binational Science Foundation.

**Th-AM-G10 PHOTOREACTIONS OF SIMPLE METAL COMPLEXES WITH DNA.**

Mindy Fleisher and Dr. Jacqueline K. Barton, Department of Chemistry, Columbia University, New York, N.Y. 10027.

In order to develop site-specific reactions of small molecules along the DNA strand, we have characterized the photochemistry of some simple coordination complexes with DNA. Several  $d^6$  metal complexes of Co(III), Rh(III) and Ru(II) were found to induce single strand scissions in closed circular DNA upon near-uv or visible light irradiation (325 and 442 nm). The  $d^3$   $\text{Cr}(\text{phen})_3^{3+}$  is inert under comparable reaction conditions. Different excited states of the metal complexes (charge transfer, intraligand, and ligand field) are all capable of inducing photoactivated strand scission. Binding modes may include intercalation, hydrogen bonding along the groove, and electrostatic association. Binding by intercalation leads to more efficient strand scission for analogous compounds. Both oxygen-dependent and oxygen-independent reactions are observed. Time resolved absorption experiments have been used to characterize the excited state intermediates. The specificity of reaction of these complexes along the DNA strand differs. The complexes should be useful for specific and non-specific cleavage of DNA both in vitro and in vivo.

**Th-AM-G11 STEREOSELECTIVITY AND REACTIVITY OF  $\text{RU}(\text{PHEN})_2\text{Cl}_2$  BOUND TO DNA**

Avis T. Danishefsky and Jacqueline K. Barton, Department of Chemistry, Columbia University, New York, N.Y. 10027.

The study of the interactions of small molecules with DNA is useful for developing chemical probes with sequence or conformational specificity. Metal complexes are particularly advantageous as spectroscopic handles, as redox active centers, and because of their coordinating ability. We have been investigating the coordination of the chiral metal complex bis(phenanthroline)dichlororuthenium(II) to DNA. Particular attention has been paid to the DNA sequence selectivity of the complex and chiral discrimination of the complex by DNA. As with other transition metal complexes, a preference for GC base pairs has been observed. Moreover the two chiral isomers differ in their affinities for the various polynucleotides examined. Whereas the  $\Lambda$  enantiomer is preferred in binding to calf thymus DNA and to the synthetic copolymer poly(dG)·poly(dC), the  $\Delta$  enantiomer is preferred in binding the alternating polymer poly(dGC)·poly(dGC). This finding suggests the presence of a common structure of the metal binding site of the first two polynucleotides different from that found in the alternating polymer. Since poly(dGC)·poly(dGC) is known to undergo transitions to Z-DNA, the effect of  $\text{Ru}(\text{phen})_2\text{Cl}_2$  on such transitions was determined.  $\text{Ru}(\text{phen})_2\text{Cl}_2$  also undergoes photoreactions with DNA. The binding is enhanced upon irradiation with visible light and DNA cleavage is observed. This photoreactivity may be useful in mapping binding sites along the strand. The binding characteristics and reactivities observed for  $\text{Ru}(\text{phen})_2\text{Cl}_2$  with DNA lend insight into the use of this and similar molecules as probes and modifiers of DNA.

**Th-AM-G12 THE DESIGN OF A CONFORMATIONALLY-SPECIFIC ARTIFICIAL NUCLEASE**

Lena A. Basile and Dr. Jacqueline K. Barton, Department of Chemistry, Columbia University, New York, N.Y. 10027.

Local conformational heterogeneities along a DNA helix may serve as necessary recognition signals for the initiation of protein-nucleic acid interactions. In an effort to probe these local differences in DNA structure chiral metal complexes have been developed, and in particular,  $\Lambda$ -tris(DIP)cobalt(III) (DIP = 4,7-diphenylphenanthroline) has been shown to cleave in a single-stranded fashion at positions which appear to demarcate the end of gene segments. Therefore, to extend the use of tris chelate metal complexes as conformationally-specific "nucleases", the complex (DIP)<sub>2</sub>(MACRO)ruthenium(II) (MACRO = 4,7-bis[N-(tris-2-amino-ethyl-amine)-p-benzene sulfonamide]-1,10-phenanthroline) has been synthesized. This reagent maintains the recognition characteristics of its analog complex,  $\text{Co}(\text{DIP})_3^{3+}$ , but now cleaves catalytically in a double-stranded fashion upon the activation of two metal-binding sites contained in the polyamine arms of the MACRO ligand. We have found that upon addition of cupric ion and  $\beta$ -mercaptoethanol, both strands of duplex DNA are efficiently cleaved. The complex may provide a unique route to cleave DNA into non-coding regions. Moreover, an understanding of how this complex interacts with DNA may serve as a simple model for protein-nucleic acid recognition and reactivity.